

# 於上行傳輸多點協調系統中利用混合型 干擾校齊之收發器設計

學生：陳琬琳

指導教授：李大嵩 博士

國立交通大學電信工程研究所碩士班

## 摘要

在蜂巢式系統下，為了使覆蓋範圍內的使用者皆能享有均勻的資料吞吐量及高傳輸速率，第三代合作夥伴(third generation partnership project; 3GPP)在前瞻長程演進系統(long term evolution-advanced; LTE-A)中提出新穎的多點協調(coordinated multipoint; CoMP)傳輸與接收技術，以提升細胞邊緣(cell-edge)使用者的服務品質(quality of service ; QoS)，進而增進系統效能。在本篇論文中，吾人於上行傳輸協調系統中引入干擾校齊(interference alignment; IA)技術，基地台之間的合作可透過後置網路(backhaul)交換資訊以達到抑制干擾的目的，進而提升系統容量。吾人提出疊代式的最大信號洩漏雜訊比(signal-to-leakage-plus-noise ratio; SLNR)干擾校齊演算法，並進一步將其與最大信號雜訊干擾比(signal-to-interference-plus-noise ratio; SINR)干擾校齊演算法結合，即為混合型干擾校齊機制。經由模擬驗證，在集中式多點協調系統的協作下，相較於傳統的方法，吾人所提出的機制具有快速收斂特性且能大幅改進系統效能。

# Mixed Criteria Interference Alignment Aided Transceiver Design in Uplink Coordinated Multipoint Systems

Student: Wan-Lin Chen

Advisor: Dr. Ta-Sung Lee

Institute of Communications Engineering

National Chiao Tung University



The demand for high data rate and uniform throughput for cellular user terminals in the cell coverage leads to a new coordinated multipoint (CoMP) transmission and reception technique proposed by the 3GPP LTE-A system. System performance can be enhanced by improving the quality of service (QoS) for cell-edge users. In this thesis, we incorporate the recently proposed interference alignment (IA) techniques in uplink CoMP to improve system capacity by leveraging the full cooperation and information exchange via the backhaul at the base stations. We propose a new iterative relaxed maximum signal-to-leakage-plus-noise ratio (SLNR) IA criterion and further combine it with the maximum signal-to-interference-plus-noise ratio (SINR) IA criterion to form a mixed-criteria IA-aided CoMP scheme. The proposed new criteria exhibit excellent convergence behaviors and provide substantial performance gain over conventional CoMP, thanks to the joint processing advantage in centralized CoMP. The effectiveness of the proposed scheme is confirmed by computer simulations.

# Acknowledgement

I would like to express my deepest gratitude to my advisor, Dr. Ta-Sung Lee, for his enthusiastic guidance and great patience. I learned a lot from his positive attitude in many areas. I also wish to thank my friends and all members in the Communication System Design and Signal Processing (CSDSP) Lab for their encouragement and help. Last but not least, I would like to show my sincere thanks to my family for their invaluable support, inspiration, and love.

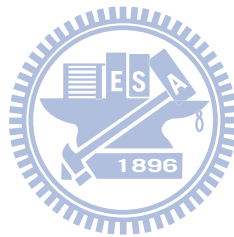
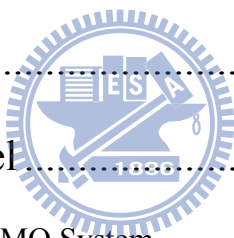
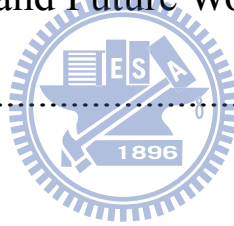


# Table of Contents

Chinese Abstract.....	i
English Abstract .....	ii
Table of Contents.....	iv
List of Figures .....	vi
List of Table.....	viii
Acronym Glossary.....	ix
Notations. ....	x
Chapter 1 Introduction.....	1
Chapter 2 System Model.....	4
2.1 Multicell Multiuser MIMO System.....	5
2.2 Channel Model.....	7
2.3 Interference Alignment .....	10
2.4 Duality Between Uplink and Downlink Transmissions.....	12
2.5 Summary.....	14
Chapter 3 Interference Alignment in Uplink Coordinated Multipoint (CoMP) Systems.....	15
3.1 Motivation.....	16
3.2 CoMP Transmission and Reception in LTE-A .....	17
3.3 Incorporation of Interference Alignment in Uplink CoMP .....	21
3.4 Channel Capacity.....	29



3.5 Computer Simulations .....	31
3.6 Summary .....	34
<b>Chapter 4 Mixed Criteria Interference Alignment in Uplink</b>	
<b>Coordinated Multipoint Systems .....</b>	<b>35</b>
4.1 Proposed Relaxed Maximum Signal-to-Leakage-plus-Noise-Ratio (SLNR) Interference Alignment Algorithm.....	36
4.2 Proposed Mixed Criteria Interference Alignment Algorithm .....	40
4.3 Complexity Analysis of Proposed Interference Alignment Algorithms .....	43
4.4 Computer Simulations .....	45
4.5 Summary .....	51
<b>Chapter 5 Conclusions and Future Works .....</b>	<b>52</b>
<b>Bibliography.....</b>	<b>55</b>



# List of Figures

<b>Figure 2–1:</b> Illustration of a multicell multiuser MIMO system.....	6
<b>Figure 2–2:</b> Transceiver design for an uplink $Q$ -cell $K$ -user MIMO system.....	6
<b>Figure 2–3:</b> MIMO configurations.....	8
<b>Figure 2–4:</b> $K$ -user interfering MIMO channel.....	10
<b>Figure 2–5:</b> Concept of IA in the spatial domain in 3-user interfering channels.....	11
<b>Figure 2–6:</b> Pictorial representation for iterative IA algorithms.....	13
<b>Figure 3–1:</b> CoMP scenario 1 [1].....	17
<b>Figure 3–2:</b> CoMP scenario 2 [1].....	18
<b>Figure 3–3:</b> CoMP scenario 3/4 [1].....	18
<b>Figure 3–4:</b> Joint transmission in downlink CoMP transmission.....	19
<b>Figure 3–5:</b> Transmission points selection in downlink CoMP transmission.....	20
<b>Figure 3–6:</b> Coordinated scheduling/beamforming in downlink CoMP transmission..	20
<b>Figure 3–7:</b> Interference rejection combining in uplink CoMP reception.....	20
<b>Figure 3–8:</b> Coordinated scheduling in uplink CoMP reception.....	20
<b>Figure 3–9:</b> Multicell multiuser MIMO system in uplink CoMP.....	22
<b>Figure 3–10:</b> Illustration of information exchange procedure with IA techniques in downlink and uplink CoMP.....	22
<b>Figure 3–11:</b> IA-aided transceiver design of a $Q$ -cell $K$ -user MIMO systems in centralized uplink CoMP.....	24
<b>Figure 3–12:</b> Simulations of $4 \times 4$ 3-cell single-user MIMO channels without CoMP.	32
<b>Figure 3–13:</b> Simulations of $4 \times 4$ 3-cell single-user MIMO channel in uplink CoMP	33

<b>Figure 4–1:</b> Rate convergence behavior of the proposed IA algorithms in uplink CoMP under i.i.d Rayleigh fading channels with no. of RP = 3, $N_t=4$ , $N_r=4$ , $K=2$ , and $d=2$ .	46
<b>Figure 4–2:</b> Rate convergence behavior of the proposed IA algorithms in uplink CoMP under highly correlated channels with no. of RP = 3, $N_t=4$ , $N_r=4$ , $K=2$ , and $d=2$ .	46
<b>Figure 4–3:</b> Sum rate performance in uplink CoMP with a MMSE receiver under i.i.d. Rayleigh channels (dashed lines: $d=1$ , solid lines: $d=2$ ) with no. of RPs = 3, $K=1$ , $N_t=4$ , $N_r=4$ , and no. of iterations=50.	47
<b>Figure 4–4:</b> Sum rate performance in uplink CoMP with a MMSE receiver under i.i.d. Rayleigh channels (dashed lines: $d=1$ , solid lines: $d=2$ ) with no. of RPs = 3, $K=2$ , $N_t=4$ , $N_r=4$ , and no. of iterations=50.	48
<b>Figure 4–5:</b> Sum rate performance in uplink CoMP with a MMSE receiver under i.i.d. Rayleigh (solid lines) and highly correlated (dashed lines) channels with no. of RPs = 3, $K=1$ , $N_t=4$ , $N_r=2$ , $d=2$ , and no. of iterations=50.	49
<b>Figure 4–6:</b> Sum rate performance in uplink CoMP with a MMSE receiver under i.i.d. Rayleigh (solid lines) and highly correlated (dashed lines) channels with no. of RPs = 3, $K=2$ , $N_t=4$ , $N_r=4$ , $d=2$ , and no. of iterations=50.	50

# List of Table

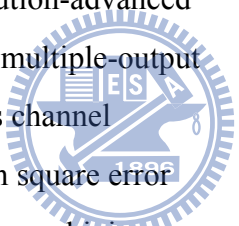
<b>Table 2-1:</b> Parameter definitions .....	7
<b>Table 2-2:</b> BS correlation matrix .....	9
<b>Table 2-3:</b> UE correlation matrix .....	9
<b>Table 2-4:</b> Different correlation levels .....	9
<b>Table 3-1:</b> Simulation parameters .....	31
<b>Table 4-1:</b> Complexity for IA criteria in uplink CoMP .....	43
<b>Table 4-2:</b> Complexity Comparison under $QN_r = N_t$ .....	44
<b>Table 4-3:</b> Sum rate enhancement comparison at SNR = 30dB .....	51





# Acronym Glossary

3GPP	third generation partnership project
AWGN	additive white Gaussian noise
BC	broadcast channel
BS	base station
CoMP	coordinated multipoint
CU	central unit
CSI	channel state information
DoF	degree of freedom
IA	interference alignment
LTE-A	long term evolution-advanced
MIMO	multiple-input-multiple-output
MAC	multiple access channel
MMSE	minimum mean square error
MRC	maximum ratio combining
QoS	quality of service
RP	reception point
RRH	remote radio head
SNR	signal-to-noise ratio
SINR	signal-to-interference-plus-noise ratio
SLNR	signal-to-leakage-plus-noise ratio
UE	user terminal
ZF	zero forcing



# Notations

$Q$	number of cells in the considered system model
$K$	number of UEs in each cell
$N_t$	number of transmit antennas
$N_r$	number of receive antennas
$\mathbf{H}_{qk}^m$	channel between the $q$ th receiver and the $k$ th UE in cell $m$
$\mathbf{V}_k^m$	precoder matrix for the $k$ th UE in cell $m$
$\mathbf{s}_k^m$	transmitted signal vector for the $k$ th UE in cell $m$
$\mathbf{n}_q$	complex Gaussian noise vector at the $q$ th receiver
$\sigma^2$	variance of complex Gaussian noise
$d$	number of total transmit data streams
$P$	transmit power constraint for a single UE
$\mathbf{U}_q$	decoder matrix at the $q$ th receiver
$\mathbf{G}_q$	linear receiver matrix at the $q$ th receiver
$R$	achievable rate
$\mathbf{X}_{(i)}$	the $i$ th column of matrix $\mathbf{X}$
$\{\mathbf{X}\}_i^j$	matrix consists of the $i$ th column to $j$ th column of matrix $\mathbf{X}$
$\text{Blkdiag}(\cdot)$	block diagonal matrix staking operator
$(\cdot)^T$	transpose operator
$(\cdot)^H$	Hermitian operator
$(\cdot)^{-1}$	inverse operation
$E\{\cdot\}$	expectation operator
$\text{tr}(\cdot)$	trace operator

# Chapter 1

## Introduction

Interference is a fundamental bottleneck in commercial mobile communications due to high density of user equipments (UEs). Unity frequency reuse has been widely adopted in the 3G/4G systems due to spectrum scarcity, and this in turn leads to severe inter-cell/intra-cell interference. On the other hand, the trend of increasing demand for higher data rate and more reliable quality of service (QoS) makes inter-cell interference management a critical issue in 4G mobile cellular networks. Multiple-input-multiple-output (MIMO) is a promising technique by exploiting spatial degrees of freedom (DoFs) to provide transmission diversity, linear capacity growth, and throughput improvement in wireless communications. To ensure uniform UE throughput and spectral efficiency in interference-limited MIMO systems, the technique of coordinated multipoint (CoMP) transmission/reception has been studied and proposed by the Third Generation Partnership Project (3GPP) for Long-Term Evolution-Advanced (LTE-A) [1].

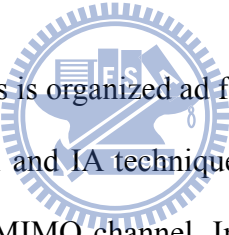
In CoMP operation, multiple transmission points coordinate with each other to receive/transmit signal from/to other points in some coordinated groups. CoMP with full cooperation exchanges full information (e.g., channel state information and decoded data) in the coordinated group via the backhaul. Centralized CoMP is a typical approach to do joint processing controlled by a central unit (CU) with collected

information in multiuser MIMO systems [2]. Some system-level evaluations have shown that CoMP transmission/reception has a significant effect on improving cell coverage, uniform QoS and throughput of cell-edge users, and spectrum efficiency [2], [3]. However, there are some challenges in CoMP implementation. First, its cooperation performance is sensitive to quantization and estimation errors in information exchange due to limited backhauling [3]-[5]. Second, the implementation cost grows with the cooperation group size because of the increased demand on the backhaul, higher complexity with more cooperating points [6], increased signaling overhead, and increased synchronization requirements, etc.

Interference alignment (IA) is a new method recently proposed to achieve the maximum spatial DoFs at high SNR in  $K$ -user interfering MIMO channels [7]. By aligning interference onto lower dimensional subspace at each receiver, the desired signal can be transmitted on interference-free dimensions to maximize the sum rate of the network. Unfortunately, there appears to be no closed-form IA solutions in multiuser MIMO systems with more than three users. Therefore, iterative approaches based on reciprocity have been employed to alternately search the best IA solutions. Several popular iterative algorithms for IA have been developed such as minimum leakage [8]-[9], maximum SINR [9], and maximum sum rate [10].

In this thesis, we propose to incorporate IA in CoMP systems, aiming to leverage the potential of both in improving overall system capacity in multiuser MIMO systems. We focus on uplink centralized CoMP reception because channel information is available at the base station (BS) without the need of resource-consuming feedback transmission, and the UEs need no modifications to support uplink CoMP. We first investigate the minimum leakage and maximum SINR IA criteria, called “leakage-IA” and “SINR-IA”, respectively. Two major findings are obtained. One is that the system performance degrades when leakage-IA is adopted in the uplink CoMP scenario; the

other is that the SLNR-IA criterion is more suitable for the transmitter than receiver. Therefore, two IA-aided transceiver designs using duality between uplink and downlink transmissions are proposed. One is the relaxed maximum signal-to-leakage-plus-noise ratio (SLNR)-IA to improve leakage-IA; the other is the mixed criteria IA which combines relaxed SLNR-IA at transmitter and SINR-IA at receiver. The iterations start with arbitrary precoders which induce a joint decoder according to the SLNR-IA/SINR-IA criteria in the uplink. The joint decoder then updates the precoders according to the relaxed SLNR-IA criterion in the virtual downlink. The procedure is executed until convergence. Compared with SINR-IA and spatial multiplexing CoMP without IA, the proposed criteria exhibit excellent convergence behaviors and provide substantial performance gain, thanks to the joint processing advantage in centralized CoMP.



The remainder of the thesis is organized as follows. Chapter 2 presents a multicell multiuser MIMO system model and IA techniques by exploiting the uplink-downlink duality in a  $K$ -user interfering MIMO channel. In Chapter 3, CoMP transmission and reception in LTE-A is introduced and we incorporate IA in the centralized uplink CoMP scenario. The proposed IA-aided criteria in the centralized uplink CoMP reception are described in Chapter 4. Numerical simulation results illustrate the advantages of the proposed IA-aided transceiver design in this chapter. Finally, we summarize the contributions of our works and give some potential future works in Chapter 5.

# Chapter 2

## System Model

In wireless communications, interference is a fundamental challenge due to high density of user equipments (UEs). Unity frequency reuse has been widely adopted due to spectrum scarcity in 3G/4G systems, which leads to severe inter-cell/intra-cell interference. Furthermore, the increasing demand for higher data rate and link reliability makes interference management a critical issue.

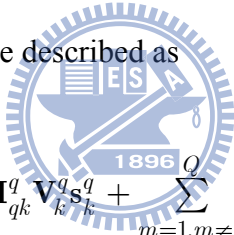
Interference management in wireless networks has been discussed for decades, and can be generally categorized as follows. First, if the interference is strong, then the interfering signal can be decoded along with the desired signal. Second, if the interference is weak, then the interfering signal can be treated as noise. Third, if the strength of interference is comparable to the desired signal, then the interference can be avoided by orthogonalizing the channel access, i.e., separating user transmissions in the time or frequency domain, leading to poor spectral efficiency. Recently, interference alignment (IA) is has been proposed as a new idea which provides good interference mitigation capability without reducing the spectral efficiency [7].

We introduce the considered uplink multicell multiuser MIMO system in Section 2.1. MIMO channel model including spatially correlated channels is described in Section 2.2. The basic concept of IA and the popular iterative IA approaches by

exploiting the uplink-downlink duality are discussed in Section 2.3 and Section 2.4, respectively. A summary of Chapter 2 is given in Section 2.5.

## 2.1 Multicell Multiuser MIMO System

Generally, a multicell multiuser MIMO system is a network containing several multiuser MIMO links sharing the same resource, and the neighboring coverage regions overlaps with each other. There are  $Q$  cells and each cell serves multiple UEs in the uplink wireless transmission, as illustrated in **Figure 2–1**. Each UE communicates only with the intended BS. Each UE and BS are equipped with  $N_t$  and  $N_r$  antennas, respectively. Each cell serves  $K$  UEs within its coverage, and the received signal at the  $q$ th BS for  $q = 1, 2, \dots, Q$  can be described as



$$\mathbf{y}_q = \sum_{k=1}^K \mathbf{H}_{qk}^q \mathbf{V}_k^q \mathbf{s}_k^q + \sum_{m=1, m \neq q}^Q \sum_{k=1}^K \mathbf{H}_{qk}^m \mathbf{V}_k^m \mathbf{s}_k^m + \mathbf{n}_q, \quad (2.1)$$

where  $\mathbf{H}_{qk}^m \in \mathbb{C}^{N_r \times N_t}$  denotes the channel between the  $q$ th receiver and the  $k$ th UE in cell  $m$ ,  $\mathbf{V}_k^m \in \mathbb{C}^{N_t \times d}$  is the precoder matrix for the  $k$ th UE in cell  $m$ ,  $\mathbf{s}_k^m \in \mathbb{C}^{d \times 1}$  is the transmitted  $d$ -layer signal vector for the  $k$ th UE in cell  $m$ , and  $\mathbf{n}_q \in \mathbb{C}^{N_r \times 1}$  represents the circularly symmetric additive white Gaussian noise (AWGN) vector with distribution  $CN(\mathbf{0}, \sigma^2 \mathbf{I})$  at the  $q$ th receiver. The transmit power for each UE is restricted to  $P$ , i.e.,  $\text{tr}(\mathbf{V}_k^m \mathbf{s}_k^m (\mathbf{s}_k^m)^H (\mathbf{V}_k^m)^H) = P$ .

After precoding and multipath propagation, the estimated transmitted signal by decoding and a linear receiver at the  $q$ th BS for  $q = 1, 2, \dots, Q$  as illustrated in **Figure 2–2** can be expressed as

$$\tilde{\mathbf{y}}_q = (\mathbf{U}_q)^H \mathbf{y}_q = (\mathbf{U}_q)^H \left( \sum_{k=1}^K \mathbf{H}_{qk}^q \mathbf{V}_k^q \mathbf{s}_k^q + \sum_{m=1, m \neq q}^Q \sum_{k=1}^K \mathbf{H}_{qk}^m \mathbf{V}_k^m \mathbf{s}_k^m + \mathbf{n}_q \right), \quad (2.2)$$

$$\hat{\mathbf{s}}_q = \mathbf{G}_q \tilde{\mathbf{y}}_q = \mathbf{G}_q (\mathbf{U}_q)^H \mathbf{y}_q, \quad (2.3)$$

where  $\mathbf{U}_q \in \mathbb{C}^{N_r \times Kd}$  denotes the decoder matrix with unit norm at the  $q$ th BS, i.e., the desired signal subspace, and  $\mathbf{G}_q \in \mathbb{C}^{Kd \times Kd}$  is the linear receiver matrix at the  $q$ th BS.

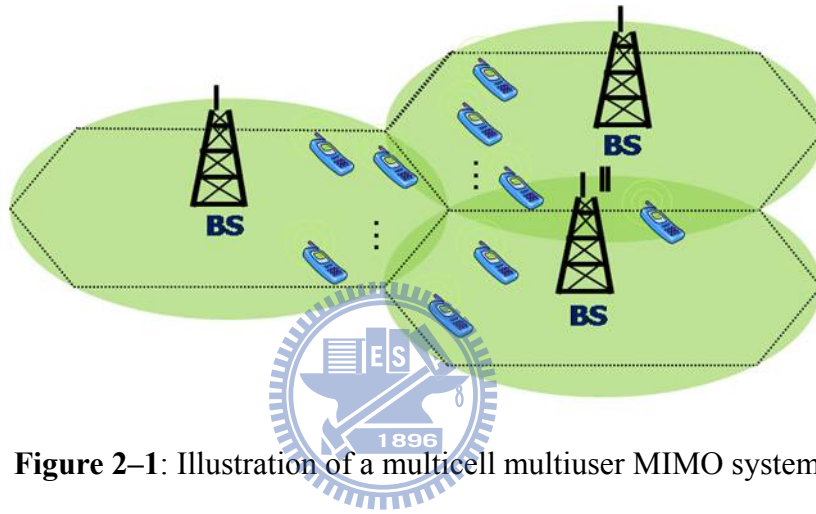


Figure 2-1: Illustration of a multicell multiuser MIMO system

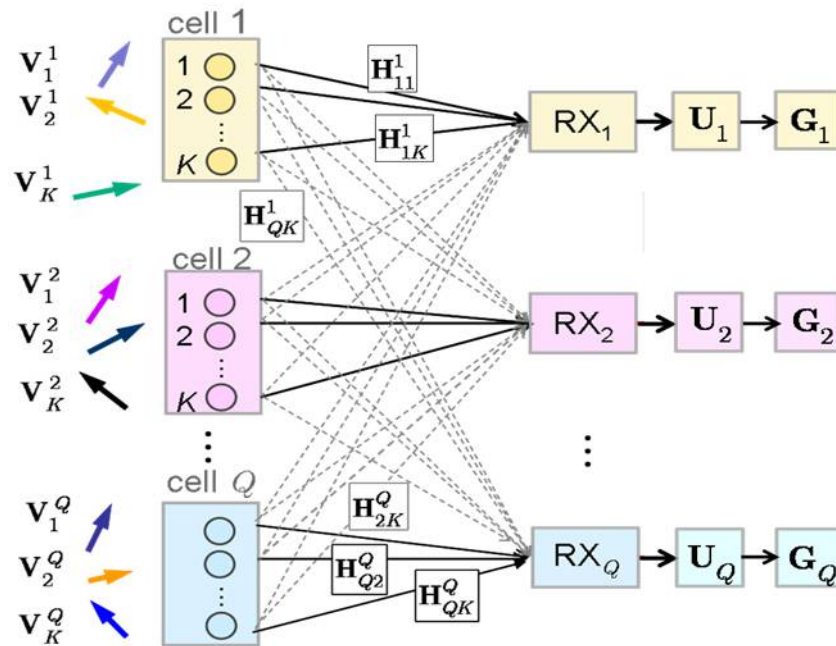


Figure 2-2: Transceiver design for an uplink  $Q$ -cell  $K$ -user MIMO system



## 2.2 Channel Model

MIMO is a promising technique by exploiting spatial degrees of freedom (DoFs) to provide transmission diversity, linear capacity growth, and throughput improvement for better link quality in most existing wireless communications. MIMO employs multiple antennas in the transmitter and receiver, and the correlation between the transmit and receive antennas is an important characteristic for practical environments. The spatial correlated MIMO fading channel model can be statistically expressed as

$$\mathbf{H}_{spat} = \mathbf{R}_r^{1/2} \mathbf{H}_{iid} \mathbf{R}_t^{1/2}, \quad (2.4)$$

or equivalently,

$$\mathbf{H}_{spat} = \text{unvec} \left\{ \mathbf{R}_{spat}^{1/2} \cdot \text{vec}(\mathbf{H}_{iid}) \right\}, \quad (2.5)$$

where the parameters are defined in Table 2-1. Generally, the independent and identically distributed Rayleigh fading channel is multiplied by a spatial correlation matrix  $\mathbf{R}_{spat}$  and becomes a spatially correlated channel.

**Table 2-1:** Parameter definitions

Parameter/function	Definition
$\mathbf{R}_t$	Spatial correlation seen from transmitter
$\mathbf{R}_r$	Spatial correlation seen from receiver
$\mathbf{H}_{iid}$	i.i.d. Rayleigh fading MIMO channel
$\text{vec}(\cdot)$	Column-wise stacking
$\text{unvec}(\cdot)$	Reverse operation of $\text{vec}(\cdot)$
$\mathbf{R}_{spat}$	$\mathbf{R}_{spat} = \mathbf{R}_t \otimes \mathbf{R}_r$ ( $\otimes$ is Kronecker product)

In this thesis, we consider the MIMO fading channels applied for the antenna configuration using uniform linear arrays at both BS and UE in uplink transmission, as illustrated in **Figure 2–3**. The MIMO channel can be expressed as

$$\mathbf{H} = \begin{bmatrix} h_{11} & h_{12} & \cdots & h_{1N_t} \\ h_{21} & h_{22} & \cdots & h_{2N_t} \\ \vdots & \vdots & \ddots & \vdots \\ h_{N_r,1} & h_{N_r,2} & \cdots & h_{N_r,N_t} \end{bmatrix}. \quad (2.6)$$

For  $\mathbf{H}_{iid}$  mentioned before, each element in Equation (2.6) is zero-mean complex Gaussian distributed, and thus the channel gain is Rayleigh distributed. The symmetric spatial correlation matrix for the transmitter (and similarly for the receiver) is defined as

$$\mathbf{R}_t = \begin{bmatrix} \rho_{11} & \rho_{12} & \cdots & \rho_{1N_t} \\ \rho_{21} & \rho_{22} & \cdots & \rho_{2N_t} \\ \vdots & \vdots & \ddots & \vdots \\ \rho_{N_t,1} & \rho_{N_t,2} & \cdots & \rho_{N_t,N_t} \end{bmatrix}, \quad (2.7)$$

where  $\rho_{ij} = \rho_{ji}^*$ , for  $i = 1, 2, \dots, N_t$ , and the diagonal components of  $\mathbf{R}_t$  correspond to the auto-correlation and are set to be one, i.e.,  $\rho_{ii} = 1$ , for  $i = 1, 2, \dots, N_t$ .

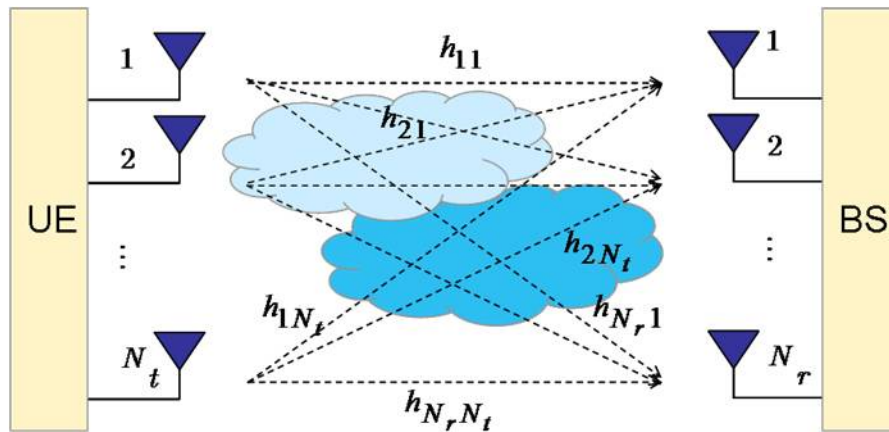


**Figure 2–3:** MIMO configurations

We adopt the correlation matrices for different MIMO configurations with different correlation levels based on [11], which are listed as follows.

**Table 2-2:** BS correlation matrix

	One antenna	Two antennas	Four antennas
<b>BS correlation</b>	$R_{BS} = 1$	$\mathbf{R}_{BS} = \begin{pmatrix} 1 & \alpha \\ \alpha^* & 1 \end{pmatrix}$	$\mathbf{R}_{BS} = \begin{pmatrix} 1 & \alpha^{1/9} & \alpha^{4/9} & \alpha \\ \alpha^{1/9*} & 1 & \alpha^{1/9} & \alpha^{4/9} \\ \alpha^{4/9*} & \alpha^{1/9*} & 1 & \alpha^{1/9} \\ \alpha^* & \alpha^{4/9*} & \alpha^{1/9*} & 1 \end{pmatrix}$

**Table 2-3:** UE correlation matrix

	One antenna	Two antennas	Four antennas
<b>UE correlation</b>	$R_{UE} = 1$	$\mathbf{R}_{UE} = \begin{pmatrix} 1 & \beta \\ \beta^* & 1 \end{pmatrix}$	$\mathbf{R}_{UE} = \begin{pmatrix} 1 & \beta^{1/9} & \beta^{4/9} & \beta \\ \beta^{1/9*} & 1 & \beta^{1/9} & \beta^{4/9} \\ \beta^{4/9*} & \beta^{1/9*} & 1 & \beta^{1/9} \\ \beta^* & \beta^{4/9*} & \beta^{1/9*} & 1 \end{pmatrix}$

**Table 2-4:** Different correlation levels

Low		Medium		High	
$\alpha$	$\beta$	$\alpha$	$\beta$	$\alpha$	$\beta$
0	0	0.3	0.9	0.9	0.9

## 2.3 Interference Alignment

IA is a new method recently emerged as a generalized multiuser MIMO techniques for  $K$ -user interfering MIMO systems, which is proven to achieve the maximum spatial DoFs at the high SNR regime [7]. The  $K$ -user interfering MIMO channel is depicted in **Figure 2–4** and can be viewed as the simplified scenario as described in Section 2.1, i.e., a  $K$ -cell single user MIMO channel. The basic idea of IA is to align or compress interference onto a lower dimension subspace at each receiver, and the desired signal can be transmitted on interference-free dimensions to maximize the sum rate of the multiuser system.

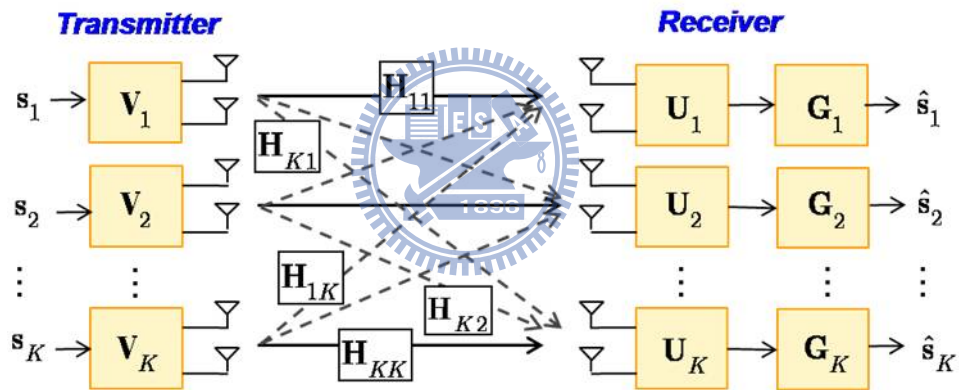


**Figure 2–4:**  $K$ -user interfering MIMO channel

Generally, IA can be categorized into the following types. First, alignment performs across frequency (or time) varying channels by frequency (or time) extensions [12]-[13]. Second, the unwanted signal is aligned on a certain subspace by exploiting the lattice code [14]-[15]. Finally, alignment performs precoding and decoding with physical multiple antennas in space domain [8]-[10], [16]. IA in the spatial domain is of our major concern in this thesis, and the main concept of IA in the spatial domain is illustrated in **Figure 2–5**.

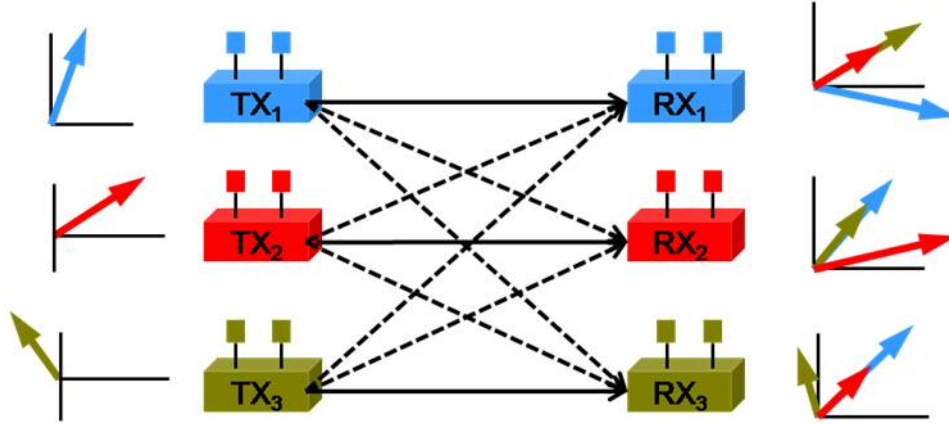


**Figure 2-5:** Concept of IA in the spatial domain in 3-user interfering channels

In  $K$ -user MIMO interfering channels, the typical IA algorithm determines a precoder matrix  $\mathbf{V}_l \in \mathbb{C}^{N_r \times d_l}$  for the  $l$ th transmitter and a decoder matrix  $\mathbf{U}_k \in \mathbb{C}^{N_r \times d_k}$  for the  $k$ th receiver, and the following conditions must be satisfied:

$$\begin{aligned} \text{rank}(\mathbf{U}_k^H \mathbf{H}_{kk} \mathbf{V}_k) &= d_k, \quad k = 1, 2, \dots, K \\ \mathbf{U}_k^H \mathbf{H}_{kl} \mathbf{V}_l &= \mathbf{0}, \quad \forall k \neq l. \end{aligned} \quad (2.8)$$

The interference is aligned onto the null space of the decoder matrix  $\mathbf{U}_k$  (for  $k = 1, 2, \dots, K$ ) whose columns are the basis of the interference-free desired signal subspace at the  $k$ th receiver. Therefore, the desired signal can be separated while the interference is completely eliminated by IA technique. Solutions for the first equality in Equation (2.8) exist if the MIMO channel is sufficiently random and the number of equations is larger or equal to the number of free variables of the equivalent channel matrix,  $\bar{\mathbf{H}} = \mathbf{U}_k^H \mathbf{H}_{kk} \mathbf{V}_k$  for  $k = 1, 2, \dots, K$ . Furthermore, the second equality in Equation (2.8) is a set of bilinear equations of the interdependent unknown precoders and decoders. A challenging issue of feasibility has been raised as to whether a system admits perfect IA or not [17].

Unfortunately, there appears to be no closed-form IA solutions in multiuser MIMO systems with more than three users. Therefore, iterative approaches based on duality between uplink and downlink transmissions have been employed to alternatively search the best IA solutions in multiuser systems. Several popular iterative IA algorithms are developed in  $K$ -user interfering MIMO channels such as minimum leakage [8]-[9], maximum SINR [9], maximum sum rate [10], and alternating minimization [16].

## 2.4 Duality Between Uplink and Downlink Transmissions

In multiuser MIMO networks, the uplink-downlink duality approach for solving the communication problems has gained a lot of attention. The duality holds when the roles of transmitters and receivers are reversed with a natural conversation of the same total transmit power. It has been studied and proven that the capacity region is the same for MAC-BC duality or point-to-point communication in MIMO (both constant and fading) channels [18]-[19].

In the  $n$ th channel use, the reciprocal MIMO channel is denoted as  $\tilde{\mathbf{H}}_{ji}[n]$  which is the reversed link (by switching the communication direction) of the channel  $\mathbf{H}_{ij}[n]$  between the  $j$ th transmitter and the  $i$ th receiver, and  $\tilde{\mathbf{H}}_{ji}[n] = (\mathbf{H}_{ij}[n])^H$ . The IA conditions for the reciprocal channel on a given interference channel use can be expressed as

$$\begin{aligned} \text{rank}\left(\tilde{\mathbf{U}}_k^H \tilde{\mathbf{H}}_{kk} \tilde{\mathbf{V}}_k\right) &= d_k, \quad k = 1, 2, \dots, K \\ \tilde{\mathbf{U}}_k^H \tilde{\mathbf{H}}_{kl} \tilde{\mathbf{V}}_l &= \mathbf{0}, \quad \forall k \neq l, \end{aligned} \quad (2.9)$$

where  $\tilde{\mathbf{V}}_k$  and  $\tilde{\mathbf{U}}_k$  represent the precoder matrix at the  $k$ th transmitter and the decoder matrix at the  $k$ th receiver in the reciprocal channel, respectively. Compared with the original interfering channels in Equation (2.8), the IA conditions are identical.

If the DoFs allocation ( $d_k$  for  $k = 1, 2, \dots, K$ ) is feasible in the original interference channel, it is also feasible in the reciprocal channel, and vice versa. The iterative approach for the best IA solutions is based on the duality characteristics by choosing the virtual precoders and virtual decoders of the reciprocal network as the decoders and precoders (respectively) of the original network. The iterations start with arbitrary precoders which induce the corresponding decoders according to IA algorithms (such as minimum leakage IA and maximum SINR IA) in the original channel. The decoders then update the precoders according to the identical IA algorithms in the reciprocal channel. The procedure is executed until convergence, as illustrated in Figure 2–6.

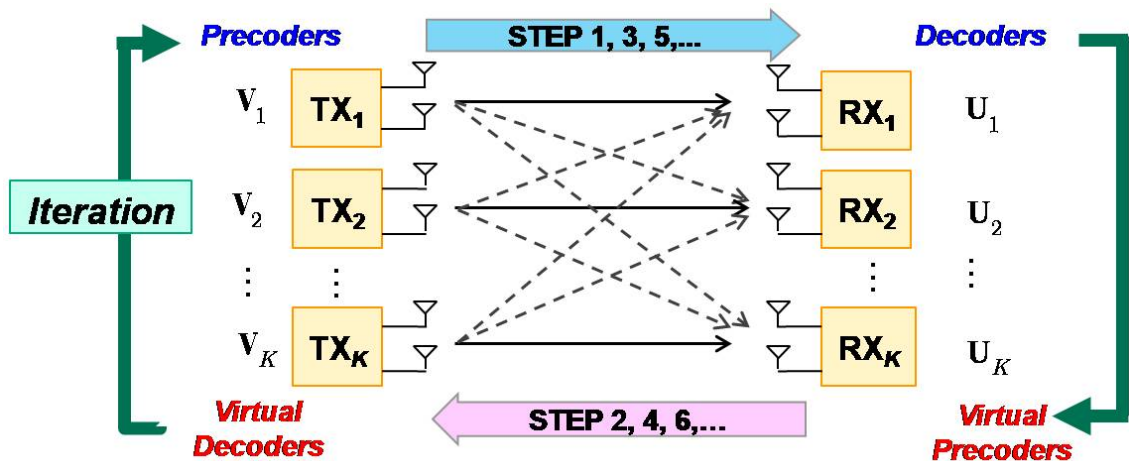
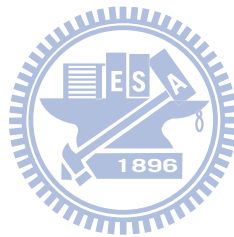


Figure 2–6: Pictorial representation for iterative IA algorithms

## 2.5 Summary

In this chapter, the multicell multiuser MIMO system in uplink transmission is presented. For dealing with such an interference-limited wireless network, IA is a recently proposed technique for improving system capacity by introducing the precoders at the transmitter side and the decoders at the receiver side in  $K$ -user interfering MIMO channels. Due to the difficulty in searching the optimal IA solutions, some popular iterative approaches for IA have been developed by exploiting the duality between the uplink and downlink transmissions. Furthermore, we describe the MIMO channel model including spatial correlated MIMO channels for practical implementation of the proposed IA-aided transceiver design.





## Chapter 3

# Interference Alignment in Uplink Coordinated Multipoint (CoMP) Systems

The fundamental demands for high link quality and high data rate have been the key features in next generation wireless communications. In 4G mobile cellular networks, it is critical to assure the fairness for uniform QoS and throughput, especially for the cell-edge users whose performance is severely limited by the interfering signals of diverse rate and strength in the neighboring cells. Therefore, CoMP transmission and reception techniques to facilitate the cooperative communication across cells are adopted as a key element by 3GPP for LTE-A [1].

In this chapter, we propose to incorporate IA in CoMP systems, aiming to leverage the potential of both in improving overall system capacity in multiuser MIMO systems. IA can be adopted in either uplink or downlink CoMP to enhance the suppression of multiuser interference. Here, we focus on the uplink CoMP scenario because channel information is available at the BSs without the need of resource-consuming feedback transmission, and the UEs need no modification to support uplink CoMP.

The organization of this chapter is as follows. Section 3.1 gives the motivation for

this work. Section 3.2 elaborates both the uplink and downlink CoMP schemes for LTE-A based on the discussion in 3GPP. The incorporation IA in the uplink CoMP scenario, and the modified minimum leakage-IA and maximum SINR-IA are investigated in Section 3.3. Channel capacity which is the key performance index in the uplink CoMP with IA adoption is introduced in Section 3.4, followed by numerical simulation results in Section 3.5. Section 3.6 summarizes this chapter.

### 3.1 Motivation

A recent information-theoretic breakthrough has been established that each user in  $K$ -user interfering MIMO channels can enjoy half the capacity of the interference free case [7]. Therefore, interference is not a fundamental limitation in such a multiuser system because it accounts for the constant scaling of the interference free case capacity, i.e., the pre-log factor of the network capacity, while the interference is sufficient mitigated. Such a surprising result is possible when IA is adopted.

CoMP is known to be a key technology for next generation mobile wireless communications; it aims to overcome the inter-cell interference to target the fairness QoS in the coverage and to improve the overall system capacity. Both IA techniques and CoMP deployments pursue for the system enhancement by dealing with the interference issue. Further, the needed information for IA implementation can be obtained via backhaul mechanism which is the critical infrastructure provided by CoMP. Therefore, we propose to incorporate IA in CoMP environments to further boost the system performance as required in LTE-A.

## 3.2 CoMP Transmission and Reception in LTE-A

CoMP transmission and reception is considered for LTE-A as a tool to improve the cell coverage, cell-edge throughput, and system efficiency. In CoMP operation, multiple points coordinate with each others to transmit signal from/to other points by backhaul mechanism in some coordinated groups; they do not incur severe interference or even can be exploited as meaningful signals.

Both uplink and downlink CoMP scenarios can be categorized into four agreed development scenarios in 3GPP [1]. Scenario 1 is the homogeneous network with intrasite CoMP, which coordinates between the cells or sectors controlled by the same BS where no backhaul connection is needed, as illustrated in **Figure 3–1**. Scenario 2 is the homogeneous network with high transmit power remote radio heads (RRHs), which coordinates between the cells belonging to different radio sites, as illustrated in **Figure 3–2**. Scenario 3/4 is the network with low power RRHs within the macrocell coverage, where the TPs or RPs created by the RRHs have the different/same cell IDs as the macro cell, as illustrated in **Figure 3–3**.

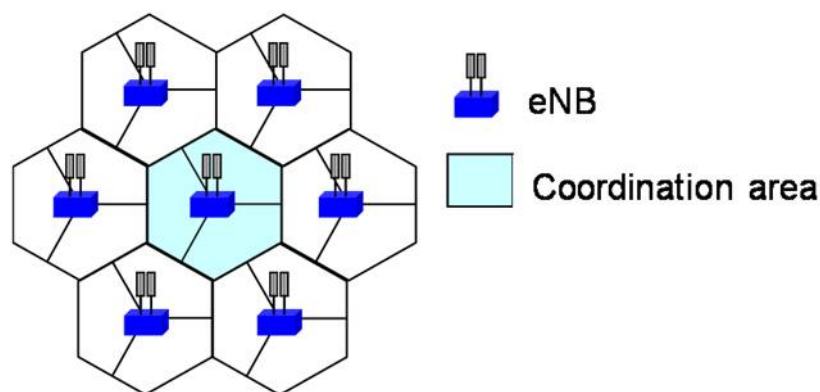


**Figure 3–1:** CoMP scenario 1 [1]

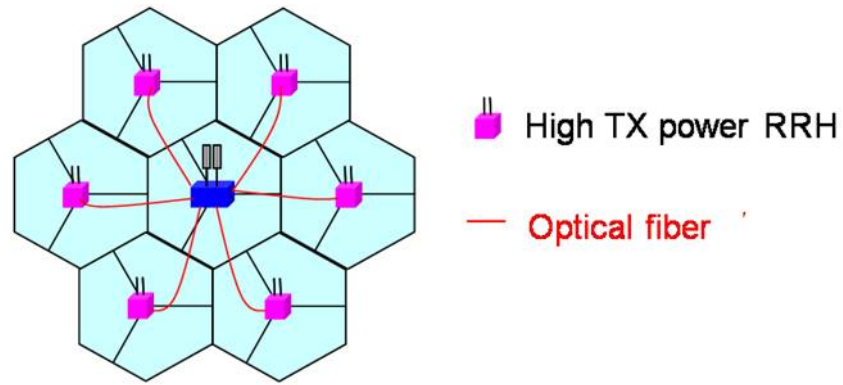


**Figure 3–2:** CoMP scenario 2 [1]

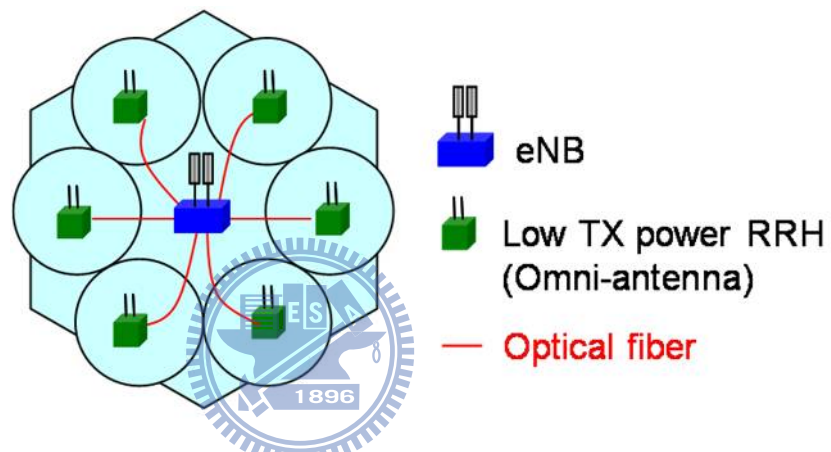


**Figure 3–3:** CoMP scenario 3/4 [1]

Centralized CoMP is a typical approach to do joint processing controlled by a central unit (CU) which can be one of the coordinated transmission/reception points (TPs/RPs) for the downlink/uplink transmissions [2]-[3]. The channel state information (CSI) and/or the data information of various links are available in the CU via backhaul, making the tremendous requirement for high speed backhauling with limited capacity. Contrary to the centralized processing, another approach which exchanges partial CSI and/or partial data information [4]-[5], called distributed CoMP, reduces the burden on backhauling by partial processing. In this thesis, the centralized CoMP with full cooperation is of our major concern.

In general, the downlink CoMP transmission schemes are classified as follows. First, each data stream is transmitted from multiple TPs at the same time to do coherent or non-coherent combining, which helps improve performance of the cell-edge users by converting the interfering signals into useful signals; this is called joint transmission as depicted in **Figure 3–4**. Second, the signal for a given user is transmitted from a TP within the coordinated group, by which the selection of the transmitted signal dynamically changes based on scheduling; this is called TP selection, as depicted in **Figure 3–5**. Third, the transmit beamforming for each user based on CSI feedback is generated to reduce the interference to other users scheduled within the coordinated group; this is called coordinated scheduling/beamforming as depicted in **Figure 3–6**. On the other hand, the uplink CoMP reception schemes are classified as follows. As shown in **Figure 3–7**, the receive weights are generated in such a way that the received signal power after combining such as minimum mean square error (MMSE) or zero forcing (ZF) at the CU is maximized; this is called interference rejection combining. As shown in **Figure 3–8**, only one user transmits at a time based on coordinated scheduling among cells with coordinated scheduling and maximum ratio combining (MRC) is typically used.

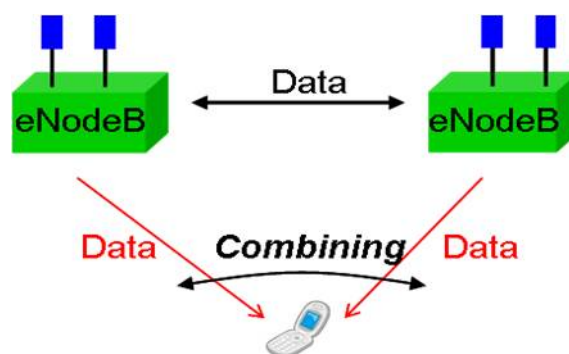


**Figure 3–4:** Joint transmission in downlink CoMP transmission

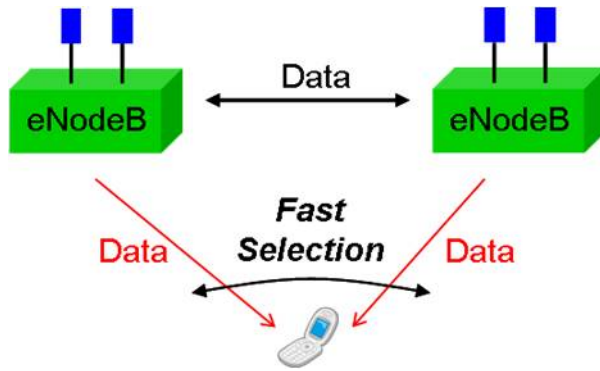


**Figure 3–5:** Transmission points selection in downlink CoMP transmission

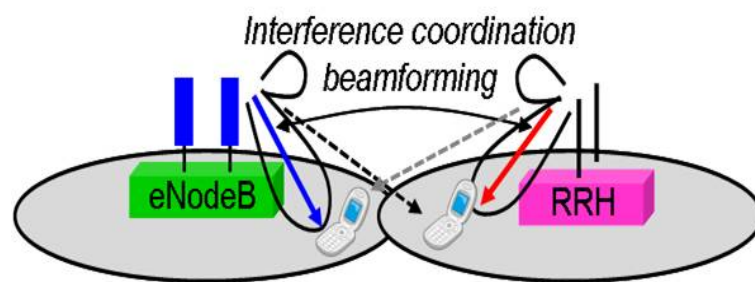


**Figure 3–6:** Coordinated scheduling/beamforming in downlink CoMP transmission

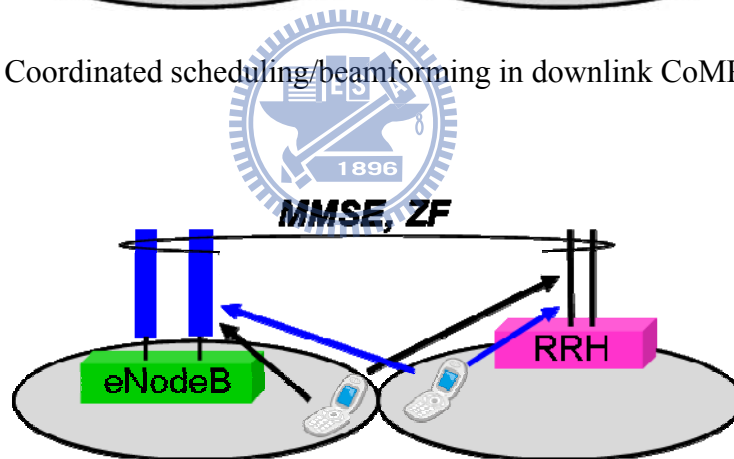


**Figure 3–7:** Interference rejection combining in uplink CoMP reception

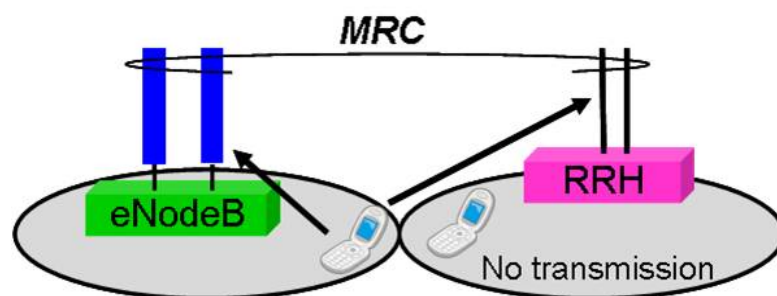


**Figure 3–8:** Coordinated scheduling in uplink CoMP reception

However, there are still some challenges to practical CoMP implementations in existing/future wireless communications. Some resources need to be reserved for the legacy users that are compliant with the earlier specifications without supporting CoMP. The cooperation performance is sensitive to the estimation and quantization errors in information exchange because of the constrained backhaul. Furthermore, the implementation cost grows with the coordinated group size due to the increased synchronization requirements and the signaling overhead, higher processing complexity, and the demand for backhaul mechanisms, and so on.

### 3.3 Incorporation of Interference Alignment in Uplink CoMP

We here introduce the IA techniques into the interfering channel model in cellular network with uplink CoMP scenario 2 involving intersite coordination between different RPs such as BSs/RRHs, i.e., the modified the multicell multiuser MIMO system mentioned in Section 2.1 as illustrated in **Figure 3–9** (which the red lines present the backhaul connections provided by CoMP).

IA can be adopted in either uplink or downlink CoMP to enhance the suppression of multiuser interference. Here, we focus on the uplink transmission because the CSI is available at the BSs without the need of resource-consuming feedback transmission (which requires less overhead for information exchange compared with the downlink case), and the UEs need no modifications to support uplink CoMP. In the uplink centralized CoMP system, cooperating BSs forward the received signals and the estimated CSI to the CU which then computes the corresponding IA precoders and the joint decoder. Therefore, the CU feeds back the IA solutions of precoders to each UE. The difference between uplink and downlink cases is depicted in **Figure 3–10**.

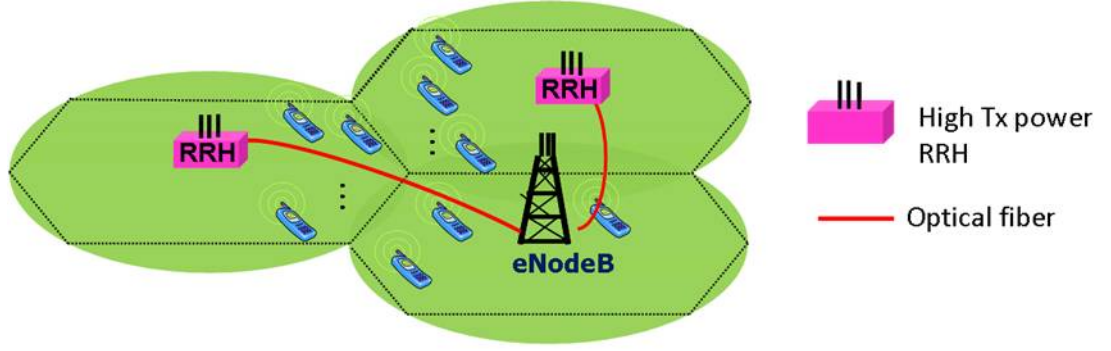


Figure 3–9: Multicell multiuser MIMO system in uplink CoMP.

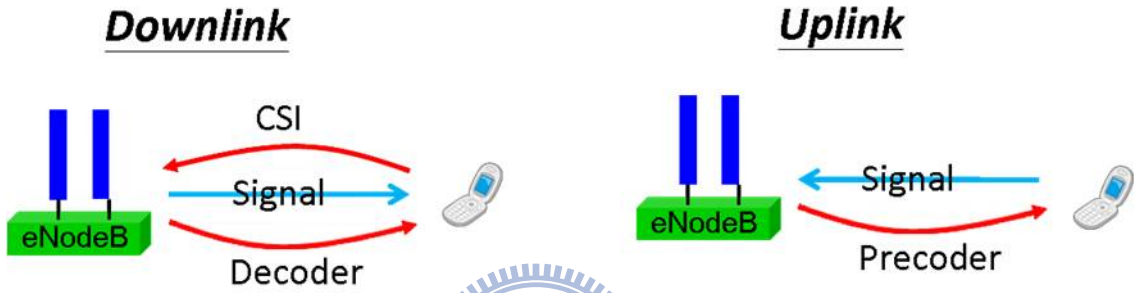


Figure 3–10: Illustration of information exchange procedure with IA techniques in downlink and uplink CoMP

Under the assumptions that negligible timing advance, perfect synchronization and channel estimation at the receivers, we consider full cooperation between the RPs in centralized uplink CoMP as illustrated in **Figure 3–11**. There are  $Q$  cells (or RPs) in coordination, and each cell serves  $K$  UEs within its coverage. All collected received signals via backhaul at the CU form the entire coordinated group can be expressed as

$$\mathbf{y} = \mathbf{H}\mathbf{V}\mathbf{s} + \mathbf{n}, \quad (3.1)$$

where  $\mathbf{y} = [\mathbf{y}_1^T, \mathbf{y}_2^T, \dots, \mathbf{y}_Q^T]^T \in \mathbb{C}^{QN_r \times 1}$ ,  $\mathbf{H} = [\mathbf{H}_{11}^1, \dots, \mathbf{H}_{1K}^1, \dots, \mathbf{H}_{11}^Q, \dots, \mathbf{H}_{1K}^Q;$

$\mathbf{H}_{21}^1, \dots, \mathbf{H}_{2K}^1, \dots, \mathbf{H}_{21}^Q, \dots, \mathbf{H}_{2K}^Q; \dots; \mathbf{H}_{Q1}^1, \dots, \mathbf{H}_{QK}^1, \dots, \mathbf{H}_{Q1}^Q, \dots, \mathbf{H}_{QK}^Q] \in \mathbb{C}^{QN_r \times QKN_t}$  where

“;” denotes the vertical concatenation of matrices,  $\mathbf{V} = \text{Blkdiag}([\mathbf{V}_1^1, \dots, \mathbf{V}_K^1, \dots,$



$\mathbf{V}_1^Q, \dots, \mathbf{V}_K^Q] \in \mathbb{C}^{QKN_t \times QKd}$  where  $\text{Blkdiag}(\cdot)$  returns a block diagonal stacking matrix,  $\mathbf{s} = [(\mathbf{s}_1^1)^T, \dots, (\mathbf{s}_K^1)^T, \dots, (\mathbf{s}_1^Q)^T, \dots, (\mathbf{s}_K^Q)^T]^T \in \mathbb{C}^{QKd \times 1}$ , and  $\mathbf{n} = [\mathbf{n}_1^T, \mathbf{n}_2^T, \dots, \mathbf{n}_Q^T]^T \in \mathbb{C}^{QN_r \times 1}$ . Then, the CU performs the centralized joint processing of the collected received signals to an equivalent MAC-like system [20]-[21]. The estimated transmitted signals by decoding and a linear receiver at the CU can be expressed as

$$\tilde{\mathbf{y}} = \mathbf{U}^H (\mathbf{H}\mathbf{V}\mathbf{s} + \mathbf{n}), \quad (3.2)$$

$$\hat{\mathbf{s}} = \mathbf{G}^H \tilde{\mathbf{y}} = \mathbf{G}^H (\bar{\mathbf{H}}\mathbf{s} + \bar{\mathbf{n}}), \quad (3.3)$$

where  $\mathbf{U} \in \mathbb{C}^{QN_r \times QKd}$ ,  $\mathbf{G}^H \in \mathbb{C}^{QKd \times QKd}$ ,  $\bar{\mathbf{H}} \in \mathbb{C}^{QKd \times QKd}$ , and  $\bar{\mathbf{n}} \in \mathbb{C}^{QKd \times 1}$  denote the joint decoder at CU, linear receiver matrix, equivalent channel with precoding and decoding, and noise after decoding with a covariance matrix  $E(\bar{\mathbf{n}}\bar{\mathbf{n}}^H) = \sigma^2 \mathbf{I}_{QKd}$ , respectively.

The coherent combining technique of IRC in uplink CoMP is considered to design the linear receiver, among which MMSE and ZF receivers are two typical approaches. For MMSE criterion, the linear receiver can be obtained as

$$\mathbf{G}_{\text{MMSE}}^H = \min_{\mathbf{G}^H} E \left\{ \left\| \mathbf{G}^H \tilde{\mathbf{y}} - \mathbf{s} \right\|^2 \right\}, \quad (3.4)$$

$$\mathbf{G}_{\text{MMSE}}^H = \left( \bar{\mathbf{H}}^H \bar{\mathbf{H}} + \sigma^2 \mathbf{I} \right)^{-1} \bar{\mathbf{H}}^H. \quad (3.5)$$

For ZF criterion,

$$\mathbf{G}_{\text{ZF}}^H \bar{\mathbf{H}} = \mathbf{I}, \quad (3.6)$$

$$\mathbf{G}_{\text{ZF}}^H = \left( \bar{\mathbf{H}}^H \bar{\mathbf{H}} \right)^{-1} \bar{\mathbf{H}}^H. \quad (3.7)$$

Taking advantages of the backhaul resource and centralized joint processing at the CU, more DoFs could be exploited for recovering the desired signals. Further, IA techniques can be incorporated to further improve the overall system throughput. For the considered system model, i.e., a  $Q$ -cell  $K$ -user MIMO system in centralized uplink CoMP, the IA conditions can be modified as follows:

$$\begin{aligned} \left( \{\mathbf{U}\}_{(k-1)d+1}^{kd} \right)^H \left( \sum_{i \neq k} \{\mathbf{H}\}_{(i-1)N_t+1}^{iN_t} \mathbf{V}^{[i]} \right) &= \mathbf{0}, \quad k \in \mathcal{K} \\ \text{rank}(\mathbf{U}^H \mathbf{H} \mathbf{V}) &= QKd, \end{aligned} \quad (3.8)$$

where  $\mathbf{U} \in \mathbb{C}^{QN_r \times QKd}$  is the received interference-free signal subspace, i.e., the joint decoder at CU. We can claim that there are total  $QK$  UEs involved in the entire coordinated reception group, i.e.,  $\mathcal{K} = \{1, 2, \dots, QK\}$ , and each UE transmits  $d$ -layer signal. The equivalent precoder is denoted as  $\mathbf{V} = \text{Blkdiag}([\mathbf{V}^{[1]}, \mathbf{V}^{[2]}, \dots, \mathbf{V}^{[QK]}]) \in \mathbb{C}^{QKN_t \times QKd}$  where the precoder of the  $k$ th UE ( $k \in \mathcal{K}$ ) is represented as  $\mathbf{V}^{[k]} \in \mathbb{C}^{N_t \times d}$ .

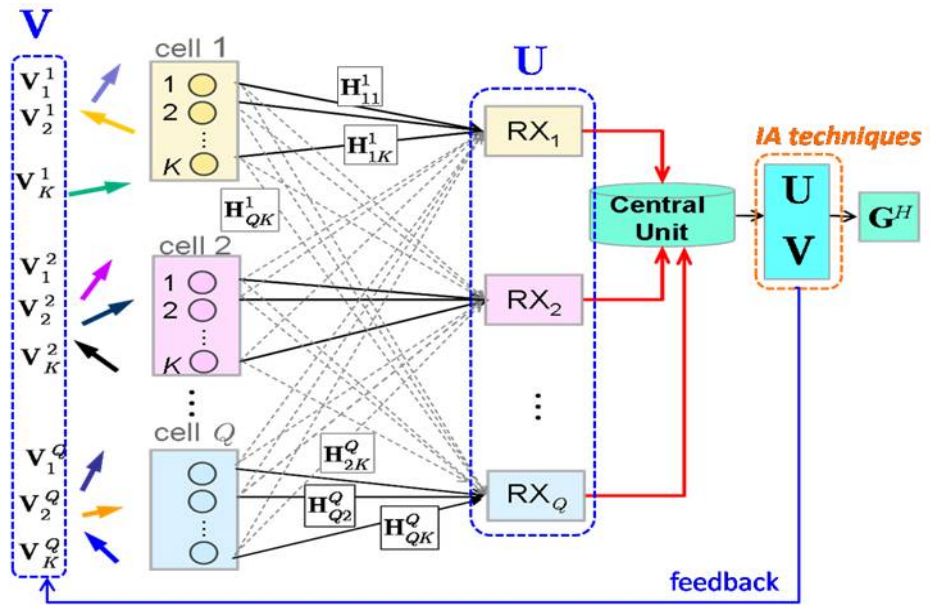


**Figure 3–11:** IA-aided transceiver design of a  $Q$ -cell  $K$ -user MIMO systems in centralized uplink CoMP

We here adopt two popular iterative IA algorithms in uplink CoMP: the minimum leakage-IA and maximum SINR-IA. Both of them were originally proposed in a  $K$ -user interfering MIMO channel [8]. The former minimizes the total interference leakage from other UEs at the current receiver after decoding, and the latter aims to maximize the received SINR at the current receiver after decoding. Based on the same concept, we can further modify the two IA algorithms by exploiting the duality between MAC and BC transmission when applied in centralized uplink CoMP.

First, the **modified minimum leakage-IA** for  $k \in \mathcal{K}$  with the precoders given in the previous iteration to compute the joint decoder at the CU is obtained below:

$$\min_{\{\mathbf{U}\}_{(k-1)d+1}^{kd}} \text{tr} \left[ (\{\mathbf{U}\}_{(k-1)d+1}^{kd})^H \mathbf{I}_k \{\mathbf{U}\}_{(k-1)d+1}^{kd} \right], \quad (3.9)$$

where

$$\mathbf{I}_k = \sum_{i=1, i \neq k}^{QK} \frac{P}{d} (\{\mathbf{H}\}_{(i-1)N_t+1}^{iN_t} \mathbf{V}^{[i]})(\{\mathbf{H}\}_{(i-1)N_t+1}^{iN_t} \mathbf{V}^{[i]})^H, \quad (3.10)$$

which yields

$$\{\mathbf{U}\}_{(k-1)d+1}^{kd} = \text{eig}_d(\mathbf{I}_k). \quad (3.11)$$

$\mathbf{I}_k \in \mathbb{C}^{QN_r \times QN_r}$  is the interference covariance matrix at the CU for the  $k$ th UE, and  $P$  is the transmit power constraint. Note that the notations  $\{\mathbf{X}\}_i^j$  and  $\text{eig}_d(\mathbf{X})$  represent a matrix consisting the  $i$ th column to the  $j$ th column of matrix  $\mathbf{X}$ , and a matrix whose columns are the eigenvectors corresponding to the  $d$  smallest eigenvalues of matrix  $\mathbf{X}$ , respectively. For updating the corresponding precoders, we consider the virtual downlink transmission, i.e., virtual BC-like transmission, with which the leakage power is minimized by setting  $\tilde{\mathbf{V}} = \mathbf{U}$ ,  $\tilde{\mathbf{U}}^{[k]} = \mathbf{V}^{[k]}$  (for  $k \in \mathcal{K}$ ), and  $\tilde{\mathbf{H}} = \mathbf{H}^H$ :

$$\min_{\tilde{\mathbf{U}}^{[k]}} \text{tr} \left[ (\tilde{\mathbf{U}}^{[k]})^H \tilde{\mathbf{I}}_k \tilde{\mathbf{U}}^{[k]} \right], \quad (3.12)$$

where

$$\tilde{\mathbf{I}}_k = \sum_{i=1, i \neq k}^{QK} \frac{P}{d} (\{\tilde{\mathbf{H}}\}^{kN_t}_{(k-1)N_t+1}) (\{\tilde{\mathbf{V}}\}^{id}_{(i-1)d+1}) (\{\tilde{\mathbf{H}}\}^{kN_t}_{(k-1)N_t+1})^H (\{\tilde{\mathbf{V}}\}^{id}_{(i-1)d+1})^H, \quad (3.13)$$

which yields

$$\tilde{\mathbf{U}}^{[k]} = \text{eig}_d(\tilde{\mathbf{I}}_k). \quad (3.14)$$

$\tilde{\mathbf{I}}_k \in \mathbb{C}^{N_t \times N_t}$  is the interference covariance matrix received at the  $k$ th UE in the reciprocal channels. The notation  $\{\mathbf{X}\}^H_i^j$  denotes a matrix consisting of the  $i$ th row to the  $j$ th row of matrix  $\mathbf{X}$ . The virtual decoders are then used as the precoders in the original network for the next iteration.

Second, we introduce the **modified maximum SINR-IA** in centralized uplink CoMP (which the procedure for IA solutions is similar to the minimum leakage-IA but with a different objective function). For the  $l$ th layer of the  $k$ th UE (for  $k \in \mathcal{K}$  and  $l \in \{1, 2, \dots, d\}$ ), the layer-wise SINR with the precoders given in the previous iteration can be calculated as

$$\max_{\mathbf{U}_{((k-1)d+l)}} \frac{\frac{P}{d} \left| (\mathbf{U}_{((k-1)d+l)})^H \{\mathbf{H}\}^{kN_t}_{(k-1)N_t+1} \mathbf{V}_{(l)}^{[k]} \right|^2}{(\mathbf{U}_{((k-1)d+l)})^H \mathbf{B}_l^{[k]} \mathbf{U}_{((k-1)d+l)}}, \quad (3.15)$$

where

$$\begin{aligned} \mathbf{B}_l^{[k]} = & \sum_{i=1}^{QK} \left( \frac{P}{d} \right) \sum_{j=1}^d (\{\mathbf{H}\}^{iN_t}_{(i-1)N_t+1} \mathbf{V}_{(j)}^{[i]}) (\{\mathbf{H}\}^{iN_t}_{(i-1)N_t+1} \mathbf{V}_{(j)}^{[i]})^H \\ & - \left( \frac{P}{d} \right) (\{\mathbf{H}\}^{kN_t}_{(k-1)N_t+1} \mathbf{V}_{(l)}^{[k]}) (\{\mathbf{H}\}^{kN_t}_{(k-1)N_t+1} \mathbf{V}_{(l)}^{[k]})^H + \sigma^2 \mathbf{I}, \end{aligned} \quad (3.16)$$

which yields

$$\mathbf{U}_{((k-1)d+l)} = \frac{(\mathbf{B}_l^{[k]})^{-1} \{\mathbf{H}\}_{(k-1)N_t+1}^{kN_t} \mathbf{V}_{(l)}^{[k]}}{\left\| (\mathbf{B}_l^{[k]})^{-1} \{\mathbf{H}\}_{(k-1)N_t+1}^{kN_t} \mathbf{V}_{(l)}^{[k]} \right\|}. \quad (3.17)$$

$\mathbf{B}_l^{[k]} \in \mathbb{C}^{QN_r \times QN_r}$  is the interference-plus-noise matrix received at the CU for the  $l$ th layer of the  $k$ th UE. The notation  $\mathbf{X}_{(i)}$  denotes the  $i$ th column of matrix  $\mathbf{X}$ . Similarly,

by setting  $\tilde{\mathbf{V}} = \mathbf{U}$ ,  $\tilde{\mathbf{U}}^{[k]} = \mathbf{V}^{[k]}$  (for  $k \in \mathcal{K}$ ), and  $\tilde{\mathbf{H}} = \mathbf{H}^H$ , we can update the precoders for the next iteration by deriving the virtual decoders:

$$\max_{\tilde{\mathbf{U}}^{[k]}} \frac{\frac{P}{d} \left| (\tilde{\mathbf{U}}_{(l)}^{[k]})^H \{(\tilde{\mathbf{H}})^H\}_{(k-1)N_t+1}^{kN_t} \tilde{\mathbf{V}}_{((k-1)d+l)} \right|^2}{(\tilde{\mathbf{U}}_{(l)}^{[k]})^H \tilde{\mathbf{B}}_l^{[k]} \tilde{\mathbf{U}}_{(l)}^{[k]}}, \quad (3.18)$$

where

$$\begin{aligned} \tilde{\mathbf{B}}_l^{[k]} &= \sum_{i=1}^{QK} \left(\frac{P}{d}\right) \sum_{j=1}^d (\{(\tilde{\mathbf{H}})^H\}_{(k-1)N_t+1}^{kN_t} \tilde{\mathbf{V}}_{((i-1)d+j)}) (\{(\tilde{\mathbf{H}})^H\}_{(k-1)N_t+1}^{kN_t} \tilde{\mathbf{V}}_{((i-1)d+j)})^H \\ &\quad - \left(\frac{P}{d}\right) (\{(\tilde{\mathbf{H}})^H\}_{(k-1)N_t+1}^{kN_t} \tilde{\mathbf{V}}_{((k-1)d+l)}) (\{(\tilde{\mathbf{H}})^H\}_{(k-1)N_t+1}^{kN_t} \tilde{\mathbf{V}}_{((k-1)d+l)})^H + \sigma^2 \mathbf{I}, \end{aligned} \quad (3.19)$$

which yields

$$\tilde{\mathbf{U}}_{(l)}^{[k]} = \frac{(\tilde{\mathbf{B}}_l^{[k]})^{-1} \{(\tilde{\mathbf{H}})^H\}_{(k-1)N_t+1}^{kN_t} \tilde{\mathbf{V}}_{((k-1)d+l)}}{\left\| (\tilde{\mathbf{B}}_l^{[k]})^{-1} \{(\tilde{\mathbf{H}})^H\}_{(k-1)N_t+1}^{kN_t} \tilde{\mathbf{V}}_{((k-1)d+l)} \right\|}. \quad (3.20)$$

$\tilde{\mathbf{B}}_l^{[k]} \in \mathbb{C}^{N_t \times N_t}$  is the interference-plus-noise covariance matrix received at the  $l$ th UE in the reciprocal channels.

The iterative procedure (which is executed until convergence) for searching IA solutions of both the minimum leakage-IA and maximum SINR-IA in centralized uplink CoMP is summarized as follows:

**Step 1:**

Start with arbitrary precoders,  $\mathbf{V}^{[k]} \in \mathbb{C}^{N_t \times d}$  for  $k \in \mathcal{K}$ .

**Step 2:**

Begin iteration procedure.

**Step 3:**

Compute the joint decoder  $\mathbf{U} \in \mathbb{C}^{Q N_r \times Q K d}$  at the CU by using the leakage-IA/SINR-IA with the precoders given in the previous step.

**Step 4:**

Compute the precoders  $\mathbf{V}^{[k]}$  for  $k \in \mathcal{K}$ , by using the leakage-IA/SINR-IA in the virtual BC-like transmission with the joint decoder obtained in the previous step.

**Step 5:**

Go back to **Step 3** until convergence.

The IA processing with joint precoder-decoder design is executed at the CU, and then the CU feeds back the corresponding precoders to the UEs in coordinated group for transmission. The desired signals can be estimated by a linear receiver at the CU and then sent back to the intended RP via backhaul mechanisms. The processing procedure is depicted in **Figure 3–11**.



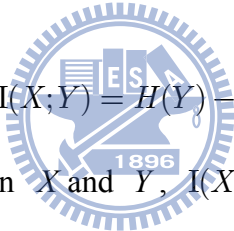
### 3.4 Channel Capacity

The channel capacity is viewed as a significant metric for multiuser MIMO systems in uplink CoMP systems with IA adoptions for the reasons: (1) its ability to capture the network throughput in a single scalar of the pre-log factor, and (2) both CoMP deployments and IA techniques pursue for overall system capacity enhancement.

Multipath propagation which can in fact contribute to capacity for a MIMO system has long been regarded as an impairment since it causes signal fading. Surprisingly, the more complicated multipath propagation is, the more capacity can be gained. The channel capacity is defined as [22]

$$C = \max_{p(x)} I(X;Y), \quad (3.21)$$

where


$$I(X;Y) = H(Y) - H(Y | X). \quad (3.22)$$

The mutual information between  $X$  and  $Y$ ,  $I(X;Y)$ , is maximized with respect to all possible transmitter statistical distributions  $p(x)$ .  $H(Y)$  and  $H(Y | X)$  are the differential entropy of  $Y$  and differential conditional entropy of  $Y$  with knowledge of  $X$  given, respectively.

For a SISO system, the ergodic channel capacity with a random complex channel gain  $h$  is given by [22]

$$C = E_H \left\{ \log \left( 1 + \frac{P}{\sigma_n^2} |h|^2 \right) \right\} \quad (\text{bps/Hz}), \quad (3.23)$$

where  $P$ ,  $\sigma_n^2$ , and  $E_H(\cdot)$  denote the transmit power, noise power, and the expectation over all channel realizations, respectively. For a MIMO system with  $N_t$  transmit

antennas and  $N_r$  receive antennas, the ergodic channel capacity of a random MIMO channel  $\mathbf{H}$  is given by [23]

$$C = \max_{\text{tr}(\mathbf{R}_x)=N_t} E_H \left\{ \log(\mathbf{I}_{N_r} + \mathbf{H}\mathbf{R}_x\mathbf{H}^H\mathbf{R}_n^{-1}) \right\} \quad (\text{bps/Hz}), \quad (3.24)$$

where  $\mathbf{R}_x = E\{\mathbf{x}\mathbf{x}^H\}$  and  $\mathbf{R}_n = E\{\mathbf{n}\mathbf{n}^H\}$  represent the correlation matrix of the transmitted signal  $\mathbf{x}$ , and the correlation matrix of the noise  $\mathbf{n}$ . Note that the total transmit power  $P$  holds constant as in SISO case such that  $\text{tr}\{\mathbf{R}_x\} = P$ . If the transmitter has no channel knowledge, the transmitted signals are chosen to be independent and equal-powered such that  $\mathbf{R}_x = (P/N_t)\mathbf{I}_{N_t}$ . Furthermore, it is common to assume uncorrelated noise at the receiver such that  $\mathbf{R}_n = \sigma_n^2\mathbf{I}_{N_r}$ . As a result, the ergodic capacity of a MIMO system can be formulated as

$$C = E_H \left\{ \log\left(\mathbf{I}_{N_r} + \frac{P}{\sigma_n^2 N_t} \mathbf{H}\mathbf{H}^H\right) \right\} \quad (\text{bps/Hz}). \quad (3.25)$$

As a performance index of the considered multicell multiuser MIMO system in uplink CoMP with IA techniques, we derive the MIMO capacity formula in terms of the summation of all estimated received signal layers after a linear receiver at the CU. The achievable total sum rate of the entire coordinated  $Q$ -cell  $K$ -user MIMO system can be expressed as [24]

$$R = E_H \left\{ \sum_{i=1}^{QKd} \log(1 + \text{SINR}_i) \right\} \quad (\text{bps/Hz}), \quad (3.26)$$

where

$$\text{SINR}_i = \frac{\mathbf{G}_{(i)} \bar{\mathbf{H}}_{(i)} \bar{\mathbf{H}}_{(i)}^H \mathbf{G}_{(i)}^H}{\sum_{j \neq i} \mathbf{G}_{(j)} \bar{\mathbf{H}}_{(j)} \bar{\mathbf{H}}_{(j)}^H \mathbf{G}_{(j)}^H + \sigma^2 \mathbf{G}_{(i)} \mathbf{G}_{(i)}^H} \quad (3.27)$$



is the received SINR for the  $i$ th layer of the estimated signals after decoding  $\mathbf{U}$  and the linear receiver  $\mathbf{G}^H$  at the CU as mentioned in Equation (3.2) and Equation (3.3). The notation  $\mathbf{A}_{(i)}$  represents the  $i$ th column of the matrix  $\mathbf{A}$ .

### 3.5 Computer Simulations

In this section, we first simulate the typical iterative IA approaches (i.e., maximum SINR and minimum leakage criteria) in a  $K$ -user interfering MIMO channels [9] (i.e., a 3-cell single-user MIMO channel without CoMP), and then incorporate the IA approaches in the uplink CoMP scenario, called ‘‘SINR-IA’’ and ‘‘leakage-IA’’, respectively. The simulation parameters used in all simulation results are listed in **Table 3-1**. A linear MMSE receiver is employed in the considered centralized uplink CoMP scenarios.

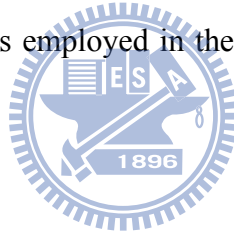


**Table 3-1:** Simulation parameters

Parameter	Value
Channel	Rayleigh fading channel
Number of transmit antennas	4
Number of receive antennas	4
Number of transmitted data streams for each UE	2
Number of cells	3
Number of UEs per cell	1
Number of channel realizations	100
Number of iterations for each IA algorithm	500

In **Figure 3–12**, the total sum rate versus SNR is evaluated in a 3-cell single-user MIMO channel without CoMP. The maximum SINR IA exhibits better sum-rate performance than minimum leakage IA and this result is consistent with [9]. Note that the definition of the total sum rate performance index in  $K$ -user interfering MIMO channels is different from that in uplink CoMP schemes [8]:

$$R = E_H \left\{ \sum_{i=1}^K \log(\det(\mathbf{I} + \text{SINR}_i)) \right\} \quad (\text{bps/Hz}), \quad (3.28)$$

where

$$\text{SINR}_i = \frac{(\mathbf{U}_i^H \mathbf{H}_{ii} \mathbf{V}_i)(\mathbf{U}_i^H \mathbf{H}_{ii} \mathbf{V}_i)^H}{\sigma^2 \mathbf{I}_d + \sum_{k \neq i} (\mathbf{U}_k^H \mathbf{H}_{ki} \mathbf{V}_i)(\mathbf{U}_k^H \mathbf{H}_{ki} \mathbf{V}_i)^H}, \quad (3.29)$$

with  $\mathbf{U}_i \in \mathbb{C}^{N_r \times d}$ ,  $\mathbf{H}_{ki} \in \mathbb{C}^{N_r \times N_t}$ , and  $\mathbf{V}_i \in \mathbb{C}^{N_t \times d}$  representing the decoder matrix for the  $i$ th receiver, the MIMO channel between the  $i$ th transmitter and the  $k$ th receiver, and the precoder matrix for the  $i$ th transmitter, respectively.

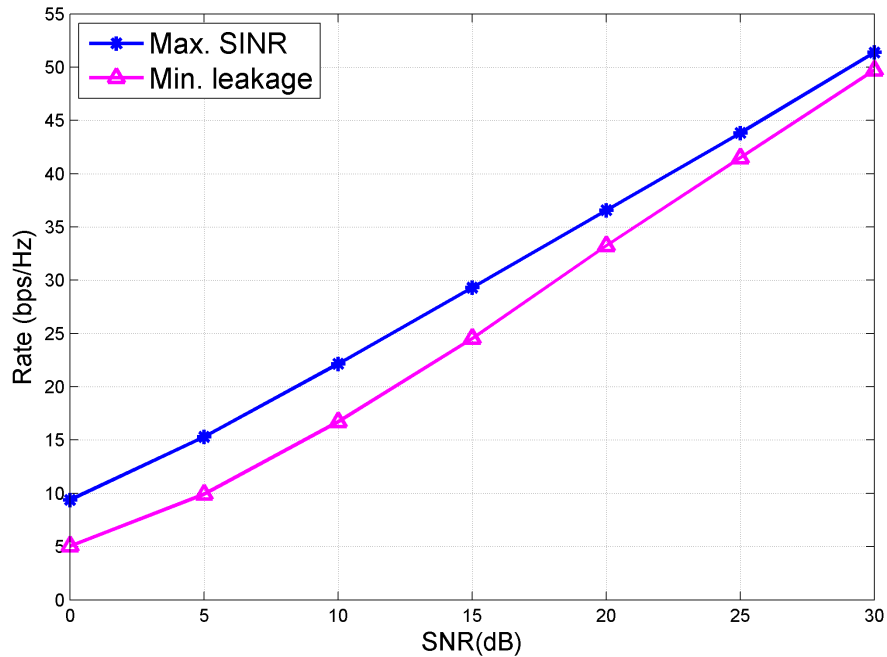


**Figure 3–12:** Simulations of  $4 \times 4$  3-cell single-user MIMO channels without CoMP

In **Figure 3–13**, the total sum rate versus SNR is evaluated for the two modified IA approaches in uplink CoMP (i.e., the leakage-IA and SINR-IA mentioned in Section 3.3). “CoMP without IA” indicates the spatial multiplexing uplink CoMP only with a MMSE receiver. SINR-IA uniformly performs better than both CoMP without IA and leakage-IA because it jointly considers the desired signal and interference to design the IA solutions (i.e., corresponding precodes for all UEs and the joint decoder at CU). The system performance degrades when the leakage-IA is adopted because leakage-IA makes no attempt to ensure the desired signals in the centralized CoMP joint design. This implies that reducing the impact on other UEs in the coordinated group without considering the desired signal power is not sufficient in uplink CoMP. This further motivates us to develop another IA-aided transceiver design in uplink CoMP which can benefit from the joint design at the CU.

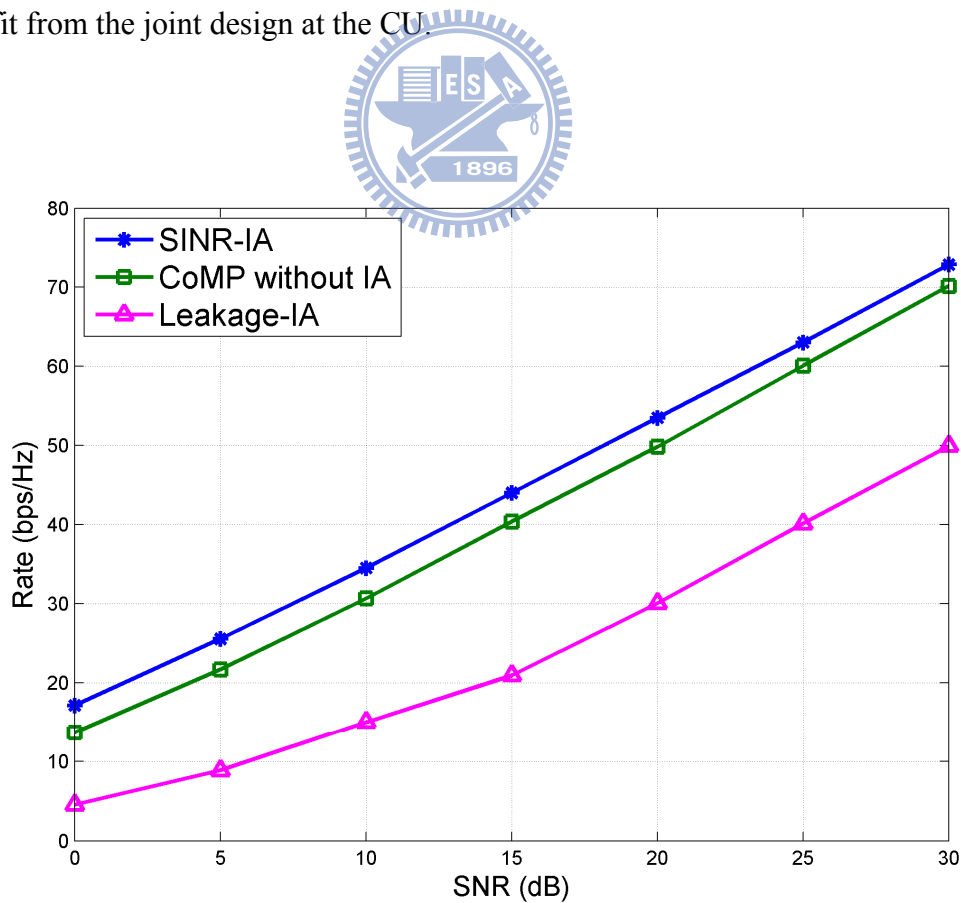


**Figure 3–13:** Simulations of  $4 \times 4$  3-cell single-user MIMO channel in uplink CoMP

## 3.6 Summary

This chapter first gives the description of both uplink and downlink CoMP scenarios and the processing schemes in 3GPP LTE-A. Both IA and CoMP target at the interference mitigation and peruse for overall system capacity enhancement; this motivates us to incorporate IA into CoMP to further enhance the system performance. Due to the feedback procedure and overhead consideration, we propose to adopt IA techniques including the minimum leakage-IA and maximum SINR-IA in uplink transmission. We observe that the leakage-IA approach does not seem to completely suppress the interference and does not benefit from the centralized uplink CoMP joint design, leading to poor performance as shown in the simulation results. Therefore, we further propose IA-aided transceiver designs in uplink CoMP by exploiting uplink-downlink duality in the next chapter.



## Chapter 4

# Mixed Criteria Interference Alignment in Uplink Coordinated Multipoint Systems

Two popular IA criteria are considered as the candidates for uplink CoMP: the minimum leakage criterion (leakage-IA) and maximum SINR criterion (SINR-IA). However, it is found that the system performance degrades when leakage-IA is adopted in uplink CoMP, and that different criteria may be used at the transmitter and receiver. Therefore, two new IA-aided transceiver designs are proposed. One is the relaxed maximum signal-to-leakage-plus-noise ratio (SLNR)-IA, which not only suppresses the total leakage power but also enhances the desired signal to improve over leakage-IA. The other is the mixed-criteria IA which combines relaxed SLNR-IA at the transmitter and SINR-IA at the receiver. The reason is that at transmitter, the precoders aim to reduce the impact on other UE transmissions without degrading the desired signal, and at the receiver, the joint decoder aims to strengthen the desired signal while suppressing interference and noise.

Due to the MAC-like nature of uplink CoMP, the iterative procedure of searching IA solutions is developed by exploiting the duality between MAC and broadcast channel (BC) transmissions [18]-[21].

This chapter is organized as follows. The proposed relaxed maximum SLNR-IA and the proposed mixed criteria IA algorithms are expressed in Section 4.1 and Section 4.2, respectively. Computational complexity analysis for the proposed IA algorithms is discussed in Section 4.3. Numerical simulation results including the convergence behaviors and the total sum rate performance are given in Section 4.4. Section 4.5 summarizes this chapter.

## 4.1 Proposed Relaxed Maximum Signal-to-Leakage-plus-Noise-Ratio (SLNR) Interference Alignment Algorithm

Under the same system parameter assumptions as mentioned in Section 3.3, the maximization of the total received SLNR at the CU for the  $Q$ -cell  $K$ -user MIMO system in centralized uplink CoMP can be formulated as

$$\begin{aligned} & \max_{\mathbf{U}, \mathbf{V}} \mathcal{J}^{\text{SLNR}}(\mathbf{U}, \mathbf{V}) \\ & \text{subject to} \quad (\mathbf{V}^{[k]})^H (\mathbf{V}^{[k]}) = \frac{P}{d} \mathbf{I}_d, \quad k \in \mathcal{K} \\ & \quad \quad \quad (\{\mathbf{U}\}_{(k-1)d+1}^{kd})^H (\{\mathbf{U}\}_{(k-1)d+1}^{kd}) = \mathbf{I}_d, \quad k \in \mathcal{K}, \end{aligned} \quad (4.1)$$

where

$$\mathcal{J}^{\text{SLNR}}(\mathbf{U}, \mathbf{V}) = \sum_{k=1}^{QK} \frac{\left\| (\{\mathbf{U}\}_{(k-1)d+1}^{kd})^H \{\mathbf{H}\}_{(k-1)N_t+1}^{kN_t} \mathbf{V}^{[k]} \right\|^2}{\text{tr} \left[ (\{\mathbf{U}\}_{(k-1)d+1}^{kd})^H \mathbf{Q}_k \{\mathbf{U}\}_{(k-1)d+1}^{kd} \right]}, \quad (4.2)$$

$$\mathbf{Q}_k = \sum_{i=1, i \neq k}^{QK} (\{\mathbf{H}\}_{(i-1)N_t+1}^{iN_t} \mathbf{V}^{[i]})(\{\mathbf{H}\}_{(i-1)N_t+1}^{iN_t} \mathbf{V}^{[i]})^H + \sigma^2 \mathbf{I}, \quad (4.3)$$

and  $\mathbf{Q}_k \in \mathbb{C}^{QN_r \times QN_r}$  is the leakage-plus-noise covariance matrix for the  $k$ th UE.

Note that the notation  $\{\mathbf{X}\}_i^j$  denotes a matrix consisting of the  $i$ th column to the  $j$ th column of matrix  $\mathbf{X}$ . To reduce the search region of precoders, each precoder is constrained to be a unitary matrix with per-layer transmit power equal to  $(P/d)$ . Moreover, the joint decoder is constrained to be a unitary matrix with unit power because the MMSE formulation in Equation (3.5) requires that the noise term is i.i.d. Gaussian distribution after decoding at the receiver.

Unfortunately, it is difficult to deal with such a complicated optimization problem due to the interdependence of the precoders and the joint decoder. Therefore, we relax the objective function in Equation (4.2) to derive a suboptimal IA solution by maximizing the SLNR of each UE for  $k \in \mathcal{K}$  as follows:

$$\begin{aligned} & \max_{\{\mathbf{U}\}_{(k-1)d+1}^{kd}, \mathbf{V}^{[k]}} \mathcal{J}_k^{\text{SLNR}}(\mathbf{U}, \mathbf{V}) \\ & \text{subject to } (\mathbf{V}^{[k]})^H (\mathbf{V}^{[k]}) = \frac{P}{d} \mathbf{I}_d, \\ & (\{\mathbf{U}\}_{(k-1)d+1}^{kd})^H (\{\mathbf{U}\}_{(k-1)d+1}^{kd}) = \mathbf{I}_d, \end{aligned} \quad (4.4)$$

where

$$\mathcal{J}_k^{\text{SLNR}}(\mathbf{U}, \mathbf{V}) = \frac{\left\| (\{\mathbf{U}\}_{(k-1)d+1}^{kd})^H \{\mathbf{H}\}_{(k-1)N_t+1}^{kN_t} \mathbf{V}^{[k]} \right\|^2}{\text{tr} \left[ (\{\mathbf{U}\}_{(k-1)d+1}^{kd})^H \mathbf{Q}_k \{\mathbf{U}\}_{(k-1)d+1}^{kd} \right]}. \quad (4.5)$$

The relaxed SLNR-IA algorithm consists of two steps. Step 1 minimizes the total received leakage-plus-noise term for  $k \in \mathcal{K}$  after decoding with precoders given in the previous iteration at the CU, i.e., the numerator in Equation (4.5). As a result, the corresponding joint decoder can be obtained as

$$\{\mathbf{U}\}_{(k-1)d+1}^{kd} = \nu_d(\mathbf{Q}_k), \quad (4.6)$$

where  $\nu_d(\mathbf{X})$  denotes a unitary matrix whose columns are the eigenvectors

corresponding to the  $d$  smallest eigenvalues of matrix  $\mathbf{X}$ . To obtain the optimal solution in Equation (4.4), Step 2 aims to update the joint decoder by maximizing the denominator in Equation (4.5) with the previous joint decoder and the same precoders given in Step 1 as follows:

$$\begin{aligned} \{\mathbf{U}\}_{(k-1)d+1}^{kd} &= \frac{\partial}{\partial \{\mathbf{U}\}_{(k-1)d+1}^{kd}} \left\| (\{\mathbf{U}\}_{(k-1)d+1}^{kd})^H \{\mathbf{H}\}_{(k-1)N_t+1}^{kN_t} \mathbf{V}^{[k]} \right\|^2 \\ &= (\{\mathbf{H}\}_{(k-1)N_t+1}^{kN_t} \mathbf{V}^{[k]}) (\{\mathbf{H}\}_{(k-1)N_t+1}^{kN_t} \mathbf{V}^{[k]})^H \{\mathbf{U}\}_{(k-1)d+1}^{kd}. \end{aligned} \quad (4.7)$$

Based on the same procedure of computing the relaxed SLNR-IA decoder, we can update the corresponding precoders by exploiting the virtual downlink transmission. As mentioned in Section 2.4,  $\tilde{\mathbf{V}} = \mathbf{U}$ ,  $\tilde{\mathbf{U}}^{[k]} = \mathbf{V}^{[k]}$  (for  $k \in \mathcal{K}$ ), and  $\tilde{\mathbf{H}} = \mathbf{H}^H$  represent the virtual joint precoder at the CU, the virtual decoder for the  $k$ th UE, and the reciprocal MIMO channel in the virtual BC-like CoMP scenario, respectively. Therefore, the virtual relaxed maximum SLNR-IA for  $k \in \mathcal{K}$  can be reformulated as

$$\begin{aligned} &\max_{\tilde{\mathbf{U}}^{[k]}, \{\tilde{\mathbf{V}}\}_{(k-1)d+1}^{kd}} \tilde{\mathcal{J}}_k^{\text{SLNR}}(\tilde{\mathbf{U}}, \tilde{\mathbf{V}}) \\ &\text{subject to} \quad (\{\tilde{\mathbf{V}}\}_{(k-1)d+1}^{kd})^H (\{\tilde{\mathbf{V}}\}_{(k-1)d+1}^{kd}) = \frac{P}{d} \mathbf{I}_d, \\ &\quad (\tilde{\mathbf{U}}^{[k]})^H (\tilde{\mathbf{U}}^{[k]}) = \mathbf{I}_d, \end{aligned} \quad (4.8)$$

where

$$\tilde{\mathcal{J}}_k^{\text{SLNR}}(\tilde{\mathbf{U}}, \tilde{\mathbf{V}}) = \frac{\left\| (\tilde{\mathbf{U}}^{[k]})^H \{(\tilde{\mathbf{H}})^H\}_{(k-1)N_t+1}^{kN_t} \{\tilde{\mathbf{V}}\}_{(k-1)d+1}^{kd} \right\|^2}{\text{tr}[(\tilde{\mathbf{U}}^{[k]})^H \tilde{\mathbf{Q}}_k \tilde{\mathbf{U}}^{[k]}]}, \quad (4.9)$$

$$\tilde{\mathbf{Q}}_k = \sum_{i=1, i \neq k}^{QK} \left( \{(\tilde{\mathbf{H}})^H\}_{(k-1)N_t+1}^{kN_t} \{\tilde{\mathbf{V}}\}_{(i-1)d+1}^{id} \right) \left( \{(\tilde{\mathbf{H}})^H\}_{(k-1)N_t+1}^{kN_t} \{\tilde{\mathbf{V}}\}_{(i-1)d+1}^{id} \right)^H + \sigma^2 \mathbf{I}, \quad (4.10)$$

and  $\tilde{\mathbf{Q}}_k \in \mathbb{C}^{N_t \times N_t}$  is the leakage-plus-noise covariance matrix received at the  $k$ th UE



in the reciprocal channels. Note that the notation  $\{(\mathbf{X})^H\}_i^j$  denotes a matrix consisting of the  $i$ th row to the  $j$ th row of matrix  $\mathbf{X}$ . According to the same procedure in the original interfering channel, the virtual decoder can be obtained with the virtual precoder given (i.e., the corresponding joint decoder in the uplink transmission,  $\tilde{\mathbf{V}} = \mathbf{U}$ ):

$$\tilde{\mathbf{U}}^{[k]} = \nu_d(\tilde{\mathbf{Q}}_k), \quad (4.11)$$

and the virtual decoder can be updated as

$$\tilde{\mathbf{U}}^{[k]} = \left( \{(\tilde{\mathbf{H}})^H\}_{(k-1)N_t+1}^{kN_t} \{\tilde{\mathbf{V}}\}_{(k-1)d+1}^{kd} \right) \left( \{(\tilde{\mathbf{H}})^H\}_{(k-1)N_t+1}^{kN_t} \{\tilde{\mathbf{V}}\}_{(k-1)d+1}^{kd} \right)^H \tilde{\mathbf{U}}^{[k]}. \quad (4.12)$$

The virtual decoders in the reciprocal network are then used as the precoders in the original network; this is the iteration procedure for searching IA solutions of the proposed relaxed maximum SLNR-IA. The procedure is executed until convergence. The procedure of the iterative relaxed SLNR-IA can be summarized as follows:

**Step 1:**

Start with arbitrary orthonormal precoders,  $\mathbf{V}^{[k]} \in \mathbb{C}^{N_t \times d}$  and  $(\mathbf{V}^{[k]})(\mathbf{V}^{[k]})^H = \mathbf{I}_d$  for  $k \in \mathcal{K}$ .

**Step 2:**

Begin iteration procedure.

**Step 3:**

Compute the joint decoder  $\mathbf{U} \in \mathbb{C}^{QN_r \times QKd}$  at the CU by using the proposed relaxed SLNR-IA algorithm with the precoders  $\mathbf{V}^{[k]}$ , for  $k \in \mathcal{K}$ , given in the previous step, i.e., from Equation (4.4) to Equation (4.7).

**Step 4:**

Compute the precoder  $\mathbf{V}^{[k]}$ , for  $k \in \mathcal{K}$ , by using the proposed relaxed SLNR-IA algorithm in the virtual BC-like transmission with the joint decoder  $\mathbf{U}$  obtained in the previous step, i.e., from Equation (4.8) to Equation (4.12).

**Step 5:**

Go back to **Step 3** until convergence.

After deriving the IA solutions with full cooperation between RPs in centralized uplink CoMP, the CU feeds back the corresponding precoders to the UEs in the coordinated group for transmission, and the desired signals can be estimated by a linear receiver processing as described in Equation (3.3).

## 4.2 Proposed Mixed Criteria Interference

### Alignment Algorithm

In this section, we further develop a mixed criteria IA in which combines the relaxed SLNR-IA is used at the transmitter and SINR-IA at the receiver. The design concept is that at the transmitter, the precoders aim to reduce the impact on other UE transmission without degrading the desired signals, and at the receiver, the joint decoder aims to strengthen the desired signals while suppressing interference and noise. The relaxed SLNR-IA part is omitted for brevity.

For the  $l$ th layer of the  $k$ th UE (for  $k \in \mathcal{K}$  and  $l \in \{1, 2, \dots, d\}$ ) in the coordinated group, the layer-wise SINR with the precoders given in the previous iteration can be calculated as

$$\begin{aligned}
& \mathbf{U}_{((k-1)d+l), \mathbf{V}^{[k]}} \max \mathcal{J}_{kl}^{\text{SINR}}(\mathbf{U}, \mathbf{V}) \\
& \text{subject to } (\mathbf{V}^{[k]})^H (\mathbf{V}^{[k]}) = \frac{P}{d} \mathbf{I}_d, \\
& \left\| \mathbf{U}_{((k-1)d+l)} \right\|^2 = 1,
\end{aligned} \tag{4.13}$$

where

$$\mathcal{J}_{kl}^{\text{SINR}}(\mathbf{U}, \mathbf{V}) = \frac{\left| (\mathbf{U}_{((k-1)d+l)})^H \{\mathbf{H}\}_{(k-1)N_t+1}^{kN_t} \mathbf{V}_{(l)}^{[k]} \right|^2}{(\mathbf{U}_{((k-1)d+l)})^H \mathbf{B}_l^{[k]} \mathbf{U}_{((k-1)d+l)}}, \tag{4.14}$$

$$\begin{aligned}
\mathbf{B}_l^{[k]} &= \sum_{i=1}^{QK} \sum_{j=1}^d (\{\mathbf{H}\}_{(i-1)N_t+1}^{iN_t} \mathbf{V}_{(j)}^{[i]}) (\{\mathbf{H}\}_{(i-1)N_t+1}^{iN_t} \mathbf{V}_{(j)}^{[i]})^H \\
&\quad - (\{\mathbf{H}\}_{(k-1)N_t+1}^{kN_t} \mathbf{V}_{(l)}^{[k]}) (\{\mathbf{H}\}_{(k-1)N_t+1}^{kN_t} \mathbf{V}_{(l)}^{[k]})^H + \sigma^2 \mathbf{I},
\end{aligned} \tag{4.15}$$

with  $\mathbf{B}_l^{[k]} \in \mathbb{C}^{QN_r \times QN_r}$  representing the interference-plus-noise covariance matrix for the  $l$ th layer of the  $k$ th UE. The notation  $\mathbf{X}_{(i)}$  denotes the  $i$ th column of matrix  $\mathbf{X}$ . Similarly, to reduce the search region of precoders, each precoder is constrained to be a unitary matrix with per-layer transmit power equal to  $(P/d)$ . Each column of the joint decoder is constrained to have unit gain for reducing the complexity in searching the solutions of the layer-wise SINR-IA criterion without changing the total power constraint at the transmitter. Therefore, we can derive the joint decoder for  $k \in \mathcal{K}$  and  $l \in \{1, 2, \dots, d\}$  given the precoders in the previous iteration, as follows:

$$\mathbf{U}_{((k-1)d+l)} = \frac{(\mathbf{B}_l^{[k]})^{-1} \{\mathbf{H}\}_{(k-1)N_t+1}^{kN_t} \mathbf{V}_{(l)}^{[k]}}{\left\| (\mathbf{B}_l^{[k]})^{-1} \{\mathbf{H}\}_{(k-1)N_t+1}^{kN_t} \mathbf{V}_{(l)}^{[k]} \right\|}. \tag{4.16}$$

Similarly, we can update the precoders based on the same procedure of the proposed relaxed SLNR-IA by exploiting the virtual BC-like transmission as mentioned in Section 4.1, i.e., from Equation (4.8) to Equation (4.12). The procedure of the

iterative mixed criteria IA can be summarized as follows:

**Step 1:**

Start with arbitrary orthonormal precoders,  $\mathbf{V}^{[k]} \in \mathbb{C}^{N_t \times d}$  and  $(\mathbf{V}^{[k]})(\mathbf{V}^{[k]})^H = \mathbf{I}_d$  for  $k \in \mathcal{K}$ .

**Step 2:**

Begin iteration procedure.

**Step 3:**

Compute the joint decoder  $\mathbf{U} \in \mathbb{C}^{QN_r \times QKd}$  at the CU by using the maximum SINR-IA algorithm with the precoders  $\mathbf{V}^{[k]}$ , for  $k \in \mathcal{K}$ , given in the previous step, i.e., from Equation (4.13) to Equation (4.16).

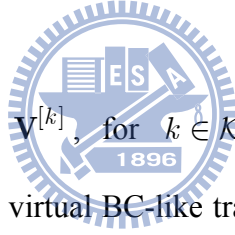
**Step 4:**

Compute the precoders  $\mathbf{V}^{[k]}$ , for  $k \in \mathcal{K}$ , by using the proposed relaxed SLNR-IA algorithm in the virtual BC-like transmission with the joint decoder  $\mathbf{U}$  obtained in the previous step, i.e., from Equation (4.8) to Equation (4.12).

**Step 5:**

Go back to **Step 3** until convergence.

Similarly, after the joint precoder-decoder design for IA, the CU feeds back the corresponding precoders to the UEs in the coordinated group for transmission, and the desired signals can be estimated by a linear receiver.



## 4.3 Complexity Analysis of Proposed Interference Alignment Algorithms

In this section, we discuss the computational complexity per iteration for the mentioned four IA criteria, i.e., minimum leakage-IA, maximum SINR-IA, maximum relaxed SLNR-IA, and mixed criteria IA. Additions are relatively cheap operations compared to multiplications or inversions, and therefore are neglected. All the computational complexity of mathematical operations is based on [25], and the overall complexity per iteration is summarized in **Table 4-1**. Generally, the complexity proportionally grows with the number of coordinated RPs and the number of UEs within each cell coverage for all cases, and is related to the MIMO configurations and the number of transmitted data streams. For  $QN_r = N_t$ , the complexity comparison of the IA criteria is listed in **Table 4-2**. Note that the computational complexity is calculated by averaging the complexity of the corresponding IA algorithm in uplink and virtual downlink.

**Table 4-1:** Complexity for IA criteria in uplink CoMP

IA criterion	Complexity
Leakage-IA	$QK\mathcal{O}(N^3)$
SINR-IA	$QKd\left(\mathcal{O}(N^3) + 0.5(QN_r + N_t)\right)$
Relaxed SLNR-IA	$QK\left(\mathcal{O}(N^3) + 8dQN_rN_t + 2d(QN_r)^2 + 2d(N_t)^2\right)$
Mixed criteria IA	$0.5QK\left[(d+1)\mathcal{O}(N^3) + dQN_r(1+8N_t) + 4d(N_t)^2\right]$

**Table 4-2:** Complexity Comparison under  $QN_r = N_t$

IA criterion	Complexity	
	$d = 1$	$\min(N_t, N_r) \geq d > 1$
I. Leakage-IA	$QK\mathcal{O}(N^3)$	$QK\mathcal{O}(N^3)$
II. SINR-IA	$QK\mathcal{O}(N^3)$	$QKd\mathcal{O}(N^3)$
III. Relaxed SLNR-IA	$QK\left(\mathcal{O}(N^3) + 12N^2\right)$	$QK\left(\mathcal{O}(N^3) + (8d + 4)N^2\right)$
IV. Mixed criteria IA	$QK\left(\mathcal{O}(N^3) + 12N^2 + N\right)$	$(1/2)QK\left((d + 1)\mathcal{O}(N^3) + 12dN^2 + dN\right)$
<b>Comparison</b>	<b>IV &gt; III &gt; II <math>\approx</math> I</b>	<b>II &gt; IV &gt; III &gt; I</b>



## 4.4 Computer Simulations

This section presents simulations of the proposed algorithms: convergence behavior evaluation and total sum rate performance comparison. For all results, we consider  $Q = 3$  coordinated RPs, and  $K$  UEs in the coverage of each RP. Each UE is equipped with  $N_t$  antennas, and each RP is equipped with  $N_r$  antennas. All UEs have the same number of transmitted signals, i.e.,  $d$  layers. Each result is obtained by averaging over 100 independent channel realizations with both i.i.d. Rayleigh fading channels and/or highly correlated channels (with spatial correlation factor of 0.9) generated applying transmit and receive antenna correlations, as mentioned in Section 2.2. 50 iterations were executed for each IA algorithm for performance evaluation. The total sum rate is calculated using the equivalent channel  $\bar{\mathbf{H}}$  in Equation (3.3) employing a linear MMSE receiver [24], as mentioned in Section 3.3.

The convergence behaviors of the proposed IA algorithms in uplink CoMP are evaluated in **Figure 4–1** and **Figure 4–2** under i.i.d. Rayleigh fading channels and highly correlated channels with  $K = 2$  and  $N_r = 4$ . The dashed lines and the solid lines denote  $\text{SNR} = 10$  dB and  $\text{SNR} = 30$  dB, respectively. As claimed, the leakage-IA performs poor in uplink CoMP as shown in **Figure 4–1** and even much poorer in correlated channels as shown in **Figure 4–2**. In general, more iterations are needed at higher SNR regime to ensure convergence. In **Figure 4–1**, the proposed mixed-criteria IA-aided CoMP scheme significantly outperforms SINR-IA and leakage-IA especially in high SNR. **Figure 4–2** reveals that the proposed IA-aided CoMP scheme exhibits robustness to highly correlated channels. In contrast, SINR-IA is quite sensitive to correlated channels, and this is particularly significant at high SNR.

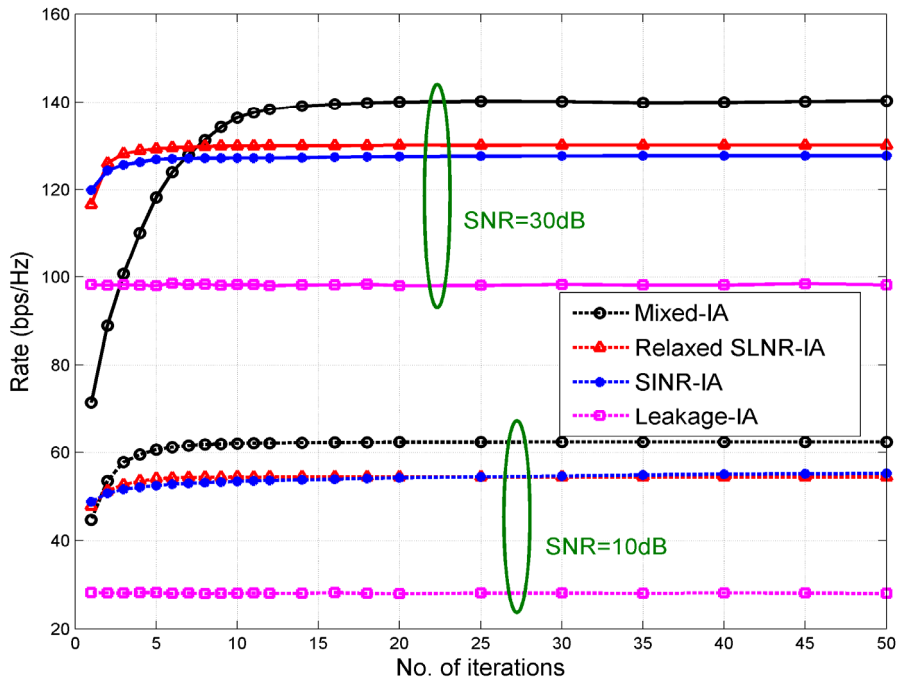


**Figure 4–1:** Rate convergence behavior of the proposed IA algorithms in uplink CoMP under i.i.d. Rayleigh fading channels with no. of RP = 3,  $N_t=4$ ,  $N_r=4$ ,  $K=2$ , and  $d=2$

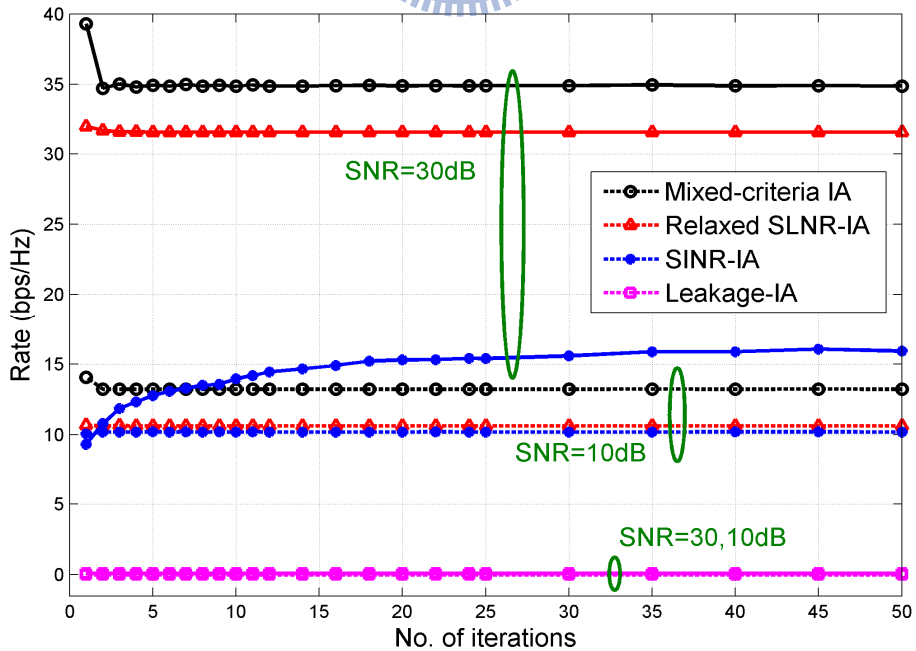


**Figure 4–2:** Rate convergence behavior of the proposed IA algorithms in uplink CoMP under highly correlated channels with no. of RP = 3,  $N_t=4$ ,  $N_r=4$ ,  $K=2$ , and  $d=2$



In **Figure 4–3**, the total sum rate versus SNR is evaluated under i.i.d. Rayleigh fading channels with  $K = 1$ ,  $N_t = 4$ , and  $N_r = 4$ . The dashed lines and the solid lines represent  $d = 1$  and  $d = 2$ , respectively. “CoMP without IA” indicates spatial multiplexing uplink CoMP only with a MMSE receiver. The sum rate performance with IA schemes for the transmitted data streams  $d = 2$  is almost twice better than  $d = 1$  since there are total twice data information transmitted in the interference-free subspace for  $d = 2$  case. The two proposed IA criteria perform better than SINR-IA and CoMP without IA schemes, and the performance gap becomes larger when each UE transmits more data streams.

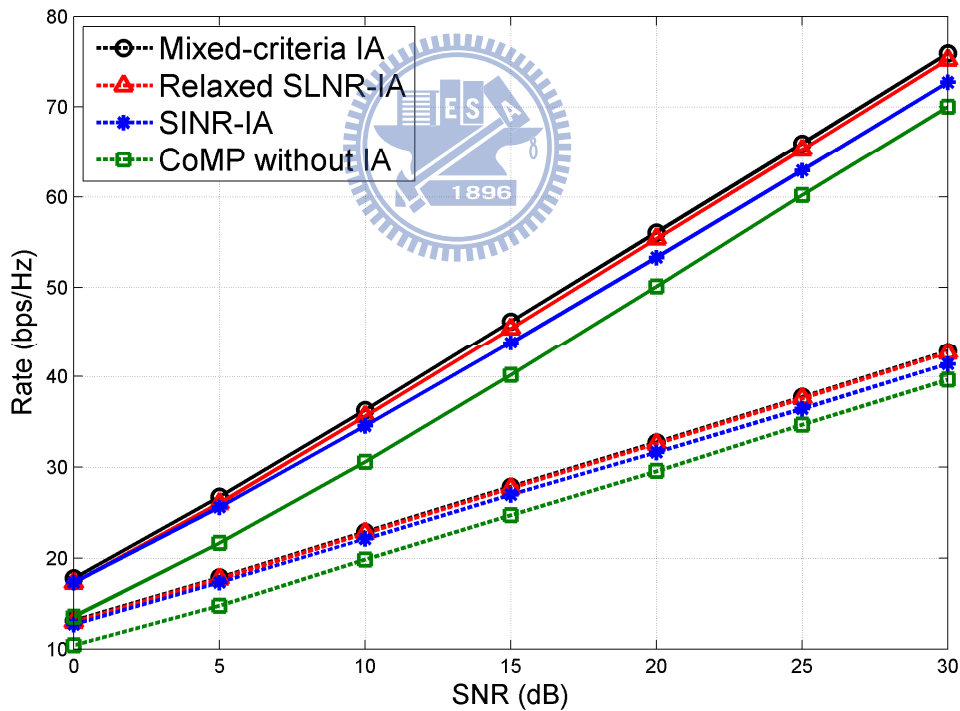


**Figure 4–3:** Sum rate performance in uplink CoMP with a MMSE receiver under i.i.d. Rayleigh channels (dashed lines:  $d=1$ , solid lines:  $d=2$ ) with no. of RPs = 3,  $K=1$ ,  $N_t=4$ ,  $N_r=4$ , and no. of iterations=50

In **Figure 4–4**, the total sum rate versus SNR is evaluated under i.i.d. Rayleigh fading channels with  $K = 2$ ,  $N_t = 4$ , and  $N_r = 4$ . The dashed lines and the solid lines represent  $d = 1$  and  $d = 2$ , respectively. Compared with **Figure 4–3**, the performance gap becomes much larger especially for more transmitted signal layers. This is because that the more UEs within the coordinated group may lead to more severe interference, but the performance can be improved thanks to IA techniques. Although the proposed relaxed SLNR-IA is comparable with SINR-IA, the proposed mixed-criteria IA significantly outperforms the other IA schemes and CoMP without IA in such the sever interference network with the more transmitted data streams and more UEs in each RP coverage. This result confirms that the proposed mixed-criteria IA provides good interference mitigation capability in the centralized uplink CoMP.

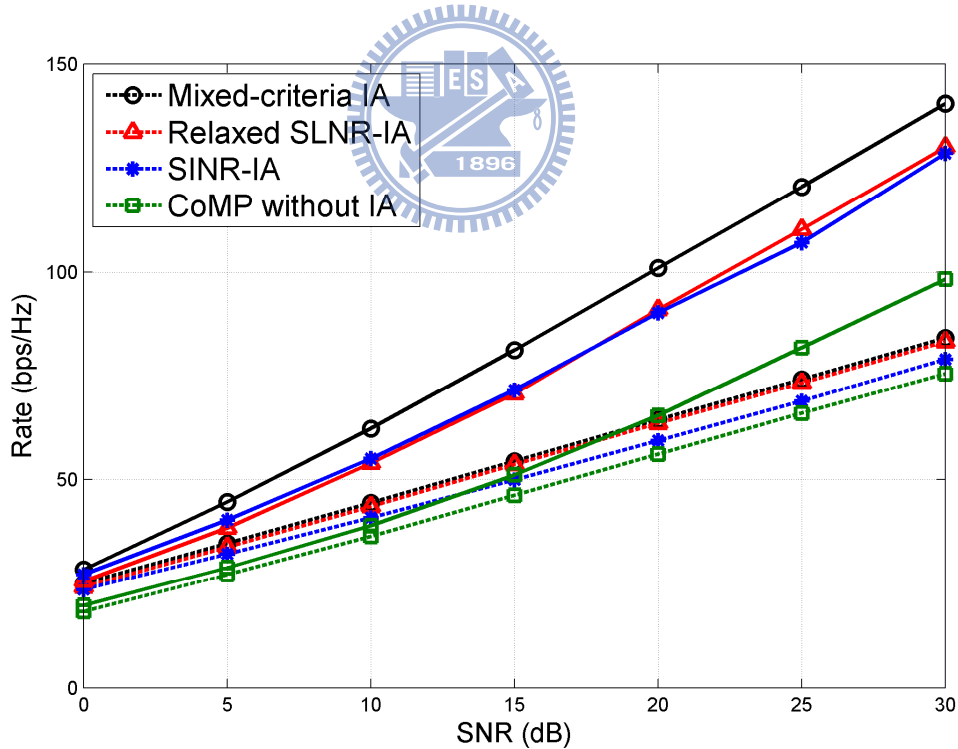


**Figure 4–4:** Sum rate performance in uplink CoMP with a MMSE receiver under i.i.d.

Rayleigh channels (dashed lines:  $d=1$ , solid lines:  $d=2$ ) with no. of RPs = 3,  $K=2$ ,

$N_t=4$ ,  $N_r=4$ , and no. of iterations=50

In **Figure 4–5**, the sum rate versus SNR is evaluated for various schemes. As expected, the system sum rate becomes worse for all IA schemes under highly correlated channels (dashed lines) compared with i.i.d. Rayleigh fading channels (solid lines) with  $K = 1$ ,  $N_t = 4$ , and  $N_r = 4$ . However, there still exists a substantial performance gap between CoMP with IA and without IA, which indicates that the proposed IA-aided uplink CoMP schemes have good interference mitigation ability and robustness to correlated channels. Overall, IA-aided CoMP transceiver design achieves uniformly better performance than CoMP without IA even when there are more total transmit antennas than receive antennas. This is because IA aligns interference onto a reduced subspace leaving more residual DoFs to recover the desired signals. Moreover, the proposed algorithms benefit from centralized CoMP joint design to achieve better performance.

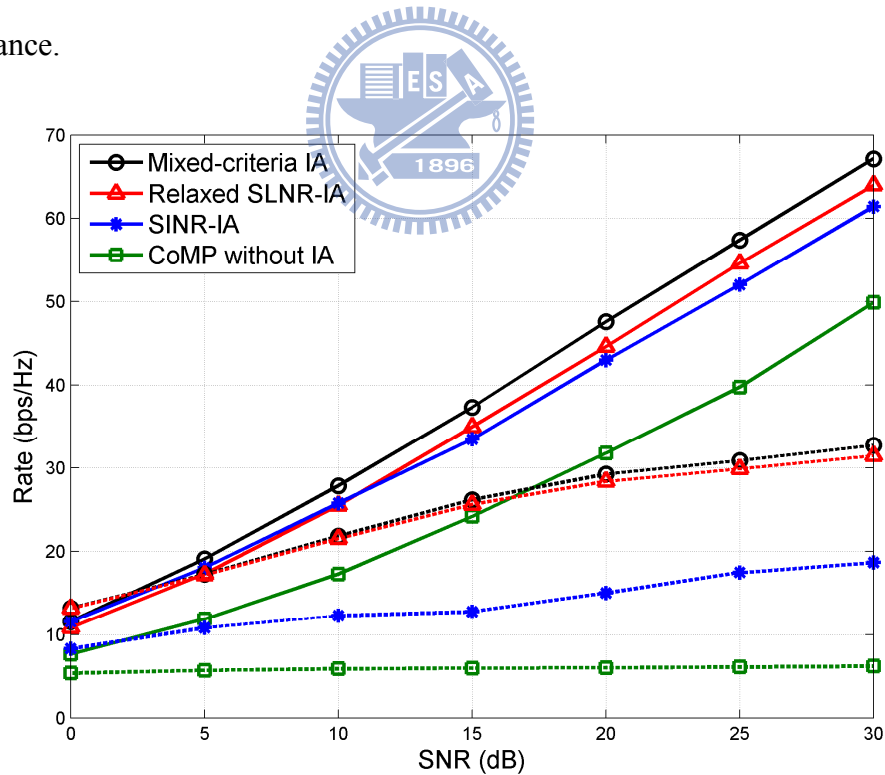


**Figure 4–5:** Sum rate performance in uplink CoMP with a MMSE receiver under i.i.d. Rayleigh (solid lines) and highly correlated (dashed lines) channels with no. of RPs = 3,

$$K=1, N_t=4, N_r=2, d=2, \text{ and no. of iterations}=50$$

In **Figure 4–6**, the sum rate is re-evaluated with  $K = 2$ ,  $N_t = 4$ , and  $N_r = 4$ . The dashed lines and the solid lines represent the highly correlated channels and i.i.d. Rayleigh fading channels, respectively. Performance enhancement under i.i.d. Rayleigh fading channels is more significant than that in **Figure 4–5** due to more receive antennas and more UEs in the coordinated group. In contrast, the performance gap becomes smaller under correlated channels. This is because that under correlated channels, the number of effective channels for data transmission and interference alignment is reduced, leading to poorer interference mitigation for IA-aided CoMP.

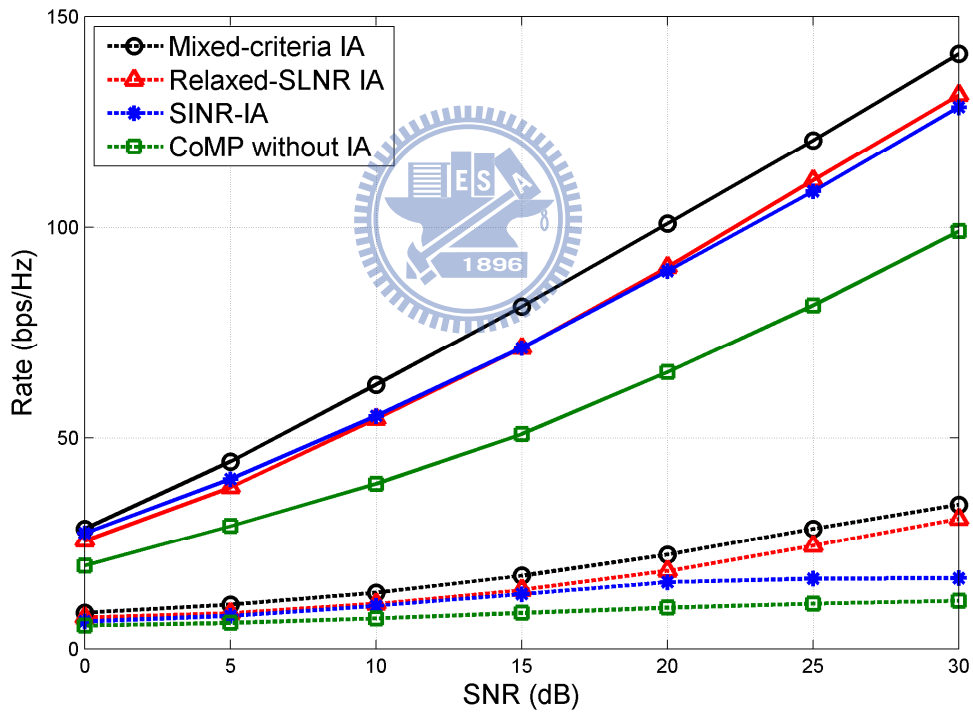


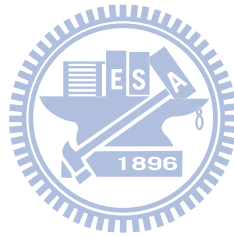
**Figure 4–6:** Sum rate performance in uplink CoMP with a MMSE receiver under i.i.d. Rayleigh (solid lines) and highly correlated (dashed lines) channels with no. of RPs = 3,

$$K=2, N_t=4, N_r=4, d=2, \text{ and no. of iterations}=50$$

The percentage sum rate enhancement of different IA-aided uplink CoMP schemes relative to conventional CoMP is compared in **Table 4-3** under different channel correlation levels at SNR = 30 dB,  $K = 2$ ,  $N_t = 4$  and  $N_r = 4$ . The result confirms that great benefits can be obtained by incorporating IA in uplink CoMP.

**Table 4-3:** Sum rate enhancement comparison at SNR = 30dB

IA in CoMP	MIMO Channel Correlation Levels		
	<i>Low</i>	<i>Medium</i>	<i>High</i>
Max. SINR-IA	28.45%	137.16%	47.38%
Relaxed SLNR-IA	31.50%	336.16%	172.49%
Mixed criteria IA	41.20%	374.95%	201.95%



## 4.5 Summary

In this chapter, considering that different design concepts should be adopted for the transmitter and receiver, two new IA criteria have been proposed, i.e., iterative relaxed maximum SLNR-IA and mixed criteria IA. They have been shown to provide good interference aligning capability and preserve more residual DoFs to recover the desired signals by a linear receiver. Simulation results confirm that the proposed algorithms exhibit better convergence behavior and achieve better sum rate performance than spatially multiplexed CoMP without IA and SINR-IA aided CoMP, especially under correlated channels.

# Chapter 5

## Conclusions and Future Works

In this thesis, to deal with severe interference due to high density of user terminals in 4G mobile cellular systems with unit frequency reuse, incorporation of the recently proposed IA techniques in uplink CoMP transceiver design with full cooperation at receiver side has been investigated. However, IA makes no attempt to consider the desired signal power within the desired signal space; this is critical on the CoMP joint design. Two new iterative IA criteria by exploiting uplink-downlink duality have been proposed in uplink CoMP, i.e., the relaxed maximum SLNR and mixed criteria IA. Both of them suppress the interference without degrading the desired signal strength and have been shown to provide good interference aligning capability by preserving more DoFs to recover the transmitted signals. Simulation results not only confirm better convergence behavior but also achieve better sum rate performance than the conventional CoMP and SINR-IA aided CoMP, even under correlated channels. The proposed IA-aided CoMP schemes represent a good candidate for 4G cellular systems for which multiuser sum rate is of a major concern.

In Chapter 2, we give a review of the multicell multiuser MIMO system in uplink transmission and express the basic concept of IA techniques by introducing precoders at transmitter and decoders at receiver. Because of the difficulty in solving the IA

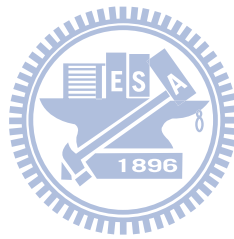
conditions, some iterative approaches for IA have been developed by utilizing the characteristic of uplink-downlink duality as described in Section 2.3 and Section 2.4.

In Chapter 3, we first give a description of both downlink and uplink CoMP schemes in 3GPP LTE-A, and then explain why we choose to incorporate IA in uplink rather than downlink transmission. The modified minimum leakage-IA and maximum SINR-IA in centralized uplink CoMP are investigated. However, it is found that the system performance degrades when leakage-IA is adopted as shown in the simulation results; this implies that it does not benefit from the joint processing at the CU when that without considering the desired signals.

Based on the concept of CoMP with IA schemes in the previous chapter, two new IA-aided transceiver designs are proposed in Chapter 4. One is the relaxed maximum SLNR-IA, which improves over the leakage-IA. It is found that the SLNR-IA criterion is more suitable for the transmitter than receiver. Therefore, the other is the mixed criteria IA which further combines the relaxed SLNR-IA at transmitter and the SINR-IA at receiver. The reason is that the precoders aim to reduce the impact on other UE transmissions without degrading the desired signals and the joint decoder aims to further strengthen the desired signals while suppressing the interference and noise. Simulations including the sum rate performance and the convergence behavior demonstrate that the proposed criteria outperform both the spatially multiplexed CoMP and SINR-IA even under the correlated channels, especially for the mixed criteria IA.

There are still some works worthy of future investigation. The first one is that the system performance can potentially be further improved by adopting successive interference cancellation technique into IA with full cooperation provided by CoMP. Moreover, quantization errors due to the limited resource and backhaul mechanisms can be addressed when designing the IA schemes. The second one is that the MIMO channel is assumed to be perfectly estimated. However, the MIMO channel cannot be

perfectly estimated in practice. Therefore, IA-aided CoMP design with robustness to channel estimation errors could be a concern. Furthermore, there is room for further improving the system performance in IA-aided transceiver design in CoMP under correlated channels. MIMO channel correlation can be considered in the design of IA algorithms.





# Bibliography

- [1] 3GPP TR36.819, “Coordinated multi-point operation for LTE physical layer aspects,” Dec. 2011.
- [2] M. Sawahashi, Y. Kishiyama, A. Morimoto, D. Nishikawa, and M. Tanno, “Coordinated multipoint transmission/reception techniques for LTE-advanced,” *IEEE Wireless Communications*, vol. 17, pp. 26-34, June 2010.
- [3] D. Lee, H. Seo, B. Clerckx, E. Hardouin, D. Mazzaresse, S. Nagata, and K. Sayana, “Coordinated multipoint transmission and reception in LTE-Advanced: deployment scenarios and operational challenges,” *IEEE Communications Magazine*, vol. 50, no. 2, pp. 148-155, Feb. 2012.
- [4] P. Marsch and G. Fettweis, “On multi-cell cooperative transmission in backhaul-constrained cellular systems,” *Annales des Télécommunications*, vol. 63, no. 5–6, May 2008.
- [5] P. Marsch and G. Fettweis, “Uplink CoMP under a constrained backhaul and imperfect channel knowledge,” *IEEE Wireless Communications*, vol. 10, no. 6, pp. 1730-1742, June 2011.
- [6] S. Das, H. Viswanathan, and G. Rittenhouse, “Dynamic load balancing through coordinated scheduling in packet data systems,” *IEEE Infocom*, San Francisco, Apr. 2003.
- [7] V. R. Cadambe, S. A. Jafar, “Interference alignment and degrees of freedom of the K-user interference channel,” *IEEE Transactions on Information Theory*, vol. 54, no. 8, pp. 3425-3441, Aug. 2008.
- [8] K. Gomadam, V. R. Cadambe, and S. A. Jafar, “Approaching the capacity of wireless networks through distributed interference alignment,” *IEEE GLOBECOM 2008*, pp. 1-6, Nov. 2008.
- [9] K. S. Gomadam, V. R. Cadambe, and S. A. Jafar, “A distributed numerical approach to interference alignment and applications to wireless interference networks,” *IEEE Transactions on Information Theory*, vol. 57, no. 6, pp. 3309-3322, June 2011.

- [10] I. Santamaria, O. Gonzalez, R. W. Heath, Jr., and S. W. Peters, "Maximum sum-rate interference alignment algorithms for MIMO channels," in *Proc. IEEE Global Telecommun. Conf.*, pp. 1-6, 2010.
- [11] 3GPP TS 36.101, "User Equipment (UE) radio transmission and reception," Mar. 2012.
- [12] L. H. Grokop, D. N. C. Tse, and R. D. Yates, "Interference alignment for line-of-sight channels," *IEEE Transactions on Information Theory*, vol. 57, no. 9, pp. 5820-5839, Sept. 2011.
- [13] M. Pischella and E. Vivier, "Comparison of distributed space and frequency interference alignment," *IEEE 21st International Symposium on PIMRC 2010*, pp. 532-537, Sept. 2010.
- [14] S. Sridharan, A. Jafarian, S. Vishwanath, S. A. Jafar, and S. Shamai, "A layered lattice coding scheme for a class of three user Gaussian interference channels," in *Proc. Allerton Conf. Commun. Ctrl. Cmpt.*, pp. 531-538, Sept. 2008.
- [15] H. Huang, V. K. N. Lau, Y. Du, and S. Liu, "Robust lattice alignment for  $K$ -user MIMO interference channels with imperfect channel knowledge," *IEEE Transactions on Signal Processing*, vol. 59, no. 7, pp. 3315-3325, July 2011.
- [16] S. W. Peters and R. W. Heath, Jr., "Interference alignment via alternating minimization," *Proc. of IEEE International Conference on Acoustics, Speech and Signal Processing*, Apr. 2009.
- [17] C. M. Yetis, G. Tiangao, S. A. Jafar, and A. H. Kayran, "On feasibility of interference alignment in MIMO interference networks," *IEEE Transactions on Signal Processing*, vol. 58, no. 9, pp. 4771-4782, Sept. 2010.
- [18] P. Viswanath and N. C. Tse, "Sum capacity of the vector Gaussian broadcast channel and uplink-downlink duality," *IEEE Transactions on Information Theory*, vol. 49, no. 8, Aug. 2003.
- [19] N. Jindal, S. Viswanath, and A. Goldsmith, "On the duality of Gaussian multiple-access and broadcast channels," *IEEE Transactions on Information Theory*, vol. 50, no. 5, May. 2004.
- [20] D. Jiang, Q. Wang, J. Liu, and C. Cui, "Uplink coordinated multi-point reception for LTE-Advanced systems," in *Proc. IEEE WiCOM*, pp.1-4, 2009.
- [21] C. Suh and D. Tse, "Interference alignment for cellular networks," in *Proc. 46th Ann. Allerton Conf. Commun.*, pp. 1037- 1044, 2008.

- [22] T. M. Cover and J. A. Thomas, *Element of Information Theory*, John Wiley & Sons, Inc., 1991.
- [23] E. Telatar, "Capacity of multi-antenna Gaussian channels," *AT&T Bell Labs Internal Tech. Memo.*, June 1995.
- [24] M. R. McKay, I. B. Collings, and A. M. Tulino, "Achievable sum rate of MIMO MMSE receivers: a general analytic framework," *IEEE Transactions on Information Theory*, vol. 56, no. 1, pp. 396-410, Jan. 2010.
- [25] G. H. Golub and C. F. V. Loan, *Matrix Computations*, Johns Hopkins University Press, 1990.

